DERIVATION OF GENERALIZED LORENZ SYSTEMS TO STUDY THE ONSET OF CHAOS IN HIGH DIMENSIONS

by

DIPANJAN ROY

Presented to the Faculty of the Graduate School of

The University of Texas at Arlington in Partial Fulfillment

of the Requirements

for the Degree of

MASTER OF SCIENCE IN PHYSICS

THE UNIVERSITY OF TEXAS AT ARLINGTON

MAY 2006

ACKNOWLEDGEMENTS

The work presented in this thesis would not have been possible without the assistance of a number of people who therefore deserve special mention. First, I would like to thank my advisor Dr. Z. E. Musielak for his constant encouragement to carry out this research. I would also like to thank Dr. John Fry and Dr. L. D. Swift for their valuable comments and suggestions which helped this research to speed up and take a more meaningful shape. I am also indebted to Dr. J. Horwitz and Dr. Alex Weiss for their support and interest to carry out this research. I am also thankful to my friends who constantly helped me with valuable advice. Finally, I would like to thank the physics department people who had been helpful throughout the completion of my papers. In particular I would like to thank Dr. Q. Zhang for showing support from time to time.

I would also like to thank my parents for their constant support in order to carry out this work and try to understand nature on the basis of exploration of fundamental physical ideas.

April 19, 2006

ABSTRACT

DERIVATION OF GENERALIZED LORENZ SYSTEMS TO STUDY THE ONSET OF CHAOS IN HIGH DIMENSIONS

Publication No. _____

DIPANJAN ROY, M.S.

The University of Texas at Arlington, 2006

Supervising Professor: Dr.Z.E.Musielak

This thesis provides a new method to derive high dimensional generalized Lorenz systems. A Lorenz system is a celebrated nonlinear dynamical dissipative system which was originally derived by Lorenz to study chaos in weather patterns. The classical two dimensional and dissipative Rayleigh-Benard convection can be approximated by Lorenz model, which was originally derived by taking into account only the lowest three Fourier modes. Numerous attempts have been made to generalize this Lorenz model as the study of this high dimensional model will pave the way to better understand the onset of chaos in high dimensional systems of current interest in

various disciplines. In this thesis a new method to extend this Lorenz model to high dimension is developed and used to construct generalized Lorenz systems. These models are constructed by selecting vertical modes, horizontal modes and finally by both vertical and horizontal modes. The principle based on which this construction is carried out is the conservation of energy in the dissipationless limit and the requirement that the models are bounded.

Finally the routes to chaos of these constructed models have been studied in great detail and an overall comparison is provided.

TABLE OF CONTENTS

LIST OF ILLUSTRATIONS

CHAPTER 1

INTRODUCTION

1.1 Historical Background

Chaos is probably the third revolution of modern physics in the last century. Other two are General Relativity and Quantum Mechanics. Low dimensional chaos is well explored territory by the beginning of this century and it's application ranges from natural and social sciences to engineering, medicine and others. Over thousands of years Man observed many regularities in nature, such as the change in seasons, and based on this observations they thought that these regularities could be predicted in a well defined manner and eventually be controlled. One of the great mathematicians Pierre Laplace who believed that if one knew the mutual positions and forces acting on all objects in Nature, one could predict all events past and future. The idea of full predictability continued until the work of French mathematician Henry Poincare (1885). He was interested in the three body problem was first to publish the observation that the future prediction of three gravitating bodies is very sensitive to the choice of initial conditions, and that under some circumstances the motion would be completely unpredictable. Unfortunately the importance of this work was not recognized for almost half a century. Around 1960 when computational facilities were introduced in science the importance of these old ideas started emerging at a remarkable speed. John Von Neumann (1952) studied how input conditions affected complex dynamical systems. He

found that a system could have points of instability. Theses are the points where small changes in the input produce enormous changes in the dynamics of the system. As a result chaotic systems show complicated behavior in space and time even if they are described by a simple physical laws and the input is primarily deterministic.

Edward Lorenz (1963) a meteorologist at MIT, studied the problem of weather prediction. He derived a set of simple nonlinear ordinary differential equations from the Saltzman (1962) model describing idealized thermal convection in the Earth's atmosphere. He showed that for a certain range of physical parameters this simple model exhibits very complicated behavior and the system is extremely sensitive to initial conditions. Therefore, the prediction of the future of the system is impossible. Lorenz pointed out that if the future prediction in a simple atmospheric convection model is impossible, then long term prediction of a complicated system such as weather, would be impossible.

1.1.1 Lorenz 3D model

The physical process that is described by Lorenz 3D model is a 2-D thermal convection, The model for convection considered by Lorenz can be represented schematically as one convective "roll" moving between two plates (see Figure 1.1). The driving force is the temperature difference (ΔT) between the two plates in the fluid. No motion is observed at low value ΔT . The transfer of heat necessary to maintain the temperature difference is achieved solely by conduction of heat. For values of ΔT greater than a critical value the necessary heat transfer cannot be achieved by

conduction alone. Therefore convective motion sets in, and this greatly increases the heat transfer. In addition to the temperature difference, the transition from a state of no motion to convective motion depends on the relative magnitude of the buoyancy and viscous forces in the fluid. One calls such a qualitative change in the flow a bifurcation. Hopf bifurcation is a type of bifurcation which generates periodic solutions. It is customary to relate this transition from conduction to convective motion to the Rayleigh number, which is a dimensionless relationship between temperature difference in the fluid and its physical properties. This need that the state of convection is known if the Rayleigh number is specified. The figure below gives a schematic idea of flow as circular convection cells.

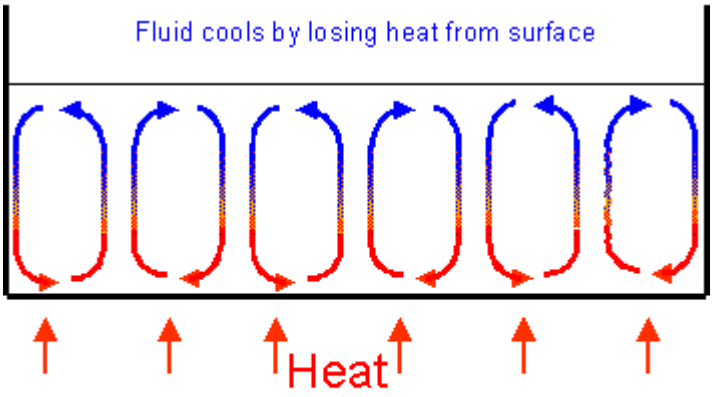

1.1 Free and forced convection

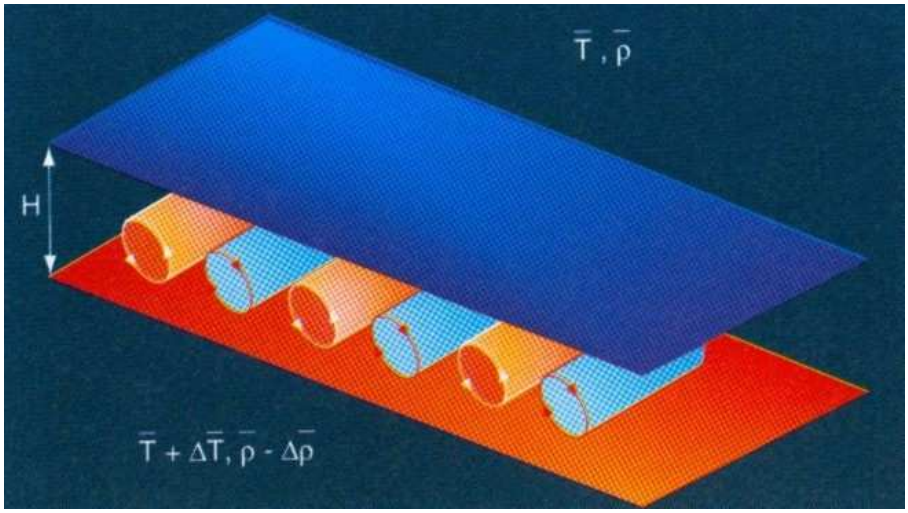

1.2 Cellular convection

The first systematic investigation of convection in shallow fluid as shown in the figure was carried out by Benard. The main result of Benard's experiment is the discovery of the steady-state, regular pattern of hexagonal convection cells. However the mechanism of selection of particular geometry is still in dispute, I would like to discuss about it in later chapters when I discuss in more detail about the selection of Fourier modes. The model in which the temperature difference is applied in the vertical direction is now called Rayleigh-Benard convection. The major difference between Benard and Rayleigh-Benard convection is that the latter is not affected by surface tension gradients. Rayleigh found trigonometric expressions describing the fluid motion and temperature departure from a state of no convection for a linearized form of the convection equations. He used this expression to investigate the onset of convection and found that it occurred when a certain quantity exceeds its critical value. This quantity is now known as the Rayleigh number. Fluid motion occurs when the Rayleigh

number, $R = g\beta H^3 \Delta T / \nu_k$, exceeds the critical Rayleigh number, $R_c = \pi^4 (1 + a^3) / a^2$. This dimensionless ratio is a parameter used to characterize the driving force ΔT in the fluid. The Rayleigh number ratio $r = R / R_c$. Where R_c depends on aspect ratio $a = (L / H)$, where g is gravity, β is the co-efficient of volume expansion, and $\nu = \mu / \rho$ and $\kappa = \alpha / \rho c_p$ are the kinematic viscosity and the co-efficient of thermal expansion respectively. For the Rayleigh-Benard convection problem, one must solve for the pressure distribution and velocity components as a function of space and time. This requires the solution of the continuity and Navier-Stokes equation describing a non – Newtonian, compressible and viscous flow. A Newtonian fluid has a linear stress-strain relationship. Compressible flow may have variation in density. Viscosity refers to the resistance to flow that a fluid has when subjected to shear stress. At this stage I would like to introduce the mathematical approach of approximating the nonlinear terms of the Navier-Stokes equations with Fourier series expansion which was first developed in 1950. Fourier series expansion is a technique in which a function is approximated in terms of a series of sines and cosines. In chapter II, I would like to show how to apply this method to original Rayleigh-Benard convection to derive Lorenz 3D model. In an effort to account for nonlinear effects in the governing equations Malkus and Veronis (1958) treated the nonlinear terms in the governing equations as perturbations of the linear convection problem. They sought steady state solutions of these nonlinear equations by expressing velocity, temperature and Rayleigh

number in the form of a power series. They concluded that the initial heat transport due to convection depends linearly on Rayleigh number and that the heat transport at higher Rayleigh number departs slightly from this linear dependence. Kuo (1961) expressed the nonlinear terms as Fourier series and the dependent variables by an infinite series of orthogonal functions. The amplitude of these functions are given as a parameter that is dependent on the Rayleigh number. For free-free boundary conditions (e.g. neglecting flow and heat transfer effects at the boundary walls) the function of all modes are sines and cosines. Thus the dependent variables can be expressed by Fourier series. Kuo's work provided a quantitative theory for the convective heat transfer as a function of temperature difference of laminar flow. Barry Saltzman(1962) generalized the ideas of kuo to time dependent finite amplitude convection. He expanded the stream function and nonlinear temperature field in terms of double Fourier series and substituted the series into the governing fluid dynamics equations, obtaining an infinite system: In this approach, the stream function is a scalar function of position and describes a steady, incompressible 2D fluid flow. To reduce an infinite system to a finite one he considered only a specific set of time dependent functions. In this thesis at later chapters I would describe my method of selecting such Fourier modes which evolve in time. They don't have spatial dependence. Saltzman integrated the system numerically to obtain time dependent solutions. Saltzman's solutions show the evolution of convection from small perturbations to finite amplitude steady-state motions for a variable Rayleigh number. He studied this system for

Rayleigh number less than ten. Saltzman concluded that for larger Rayleigh numbers fluid motion is characterized by oscillatory, overstable cellular motions. (see Figure 1.3)

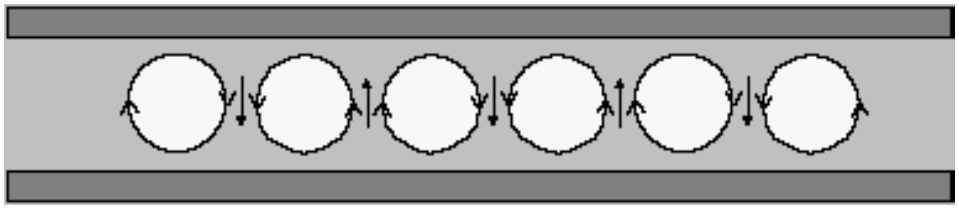

1.3 Circulation of rolls

1.1.2 Lorenz nonlinear convection model

Lorenz simplified Saltzman's model to a system of three nonlinear ordinary differential equation by retaining only three modes in Fourier series expansion. These equations represent a highly truncated two dimensional description of Rayleigh –Benard convection. He immediately realized that for a certain parameter values the solutions to his system were greatly affected by small change in initial conditions.

Lorenz's system attracted little attention until the 1971 work by Ruelle,Takens and Newhouse (Ruelle,D., (1971)) who demonstrated that turbulence in fluids would appear under few bifurcations unlike the scenario predicted by Landau (L.D.Landau (1944)). The Ruelle, Takens and Newhouse route to turbulence is much shorter than the popular theory at that time (Landau), which suggested that the chaotic state was approached after an infinite number of Hopf bifurcations. Ruelle, Takens and

Newhouse showed that only three Hopf bifurcations are required for transitions from regular to apparent chaotic behavior. The Lorenz system received enormous interest at that time, since it was the first deterministic model of a physical system that followed the proposed route to turbulence. In the same year realizing the importance of the low dimensional model J.H.Curry(1978) one of the mathematician working with Lorenz at MIT followed Saltzman's approach and extended the Lorenz system to 14 dimensions. He concluded that the gross features of the strange attractor in his system are similar to that observed in Lorenz system, however the unstable stationary solutions are replaced by tori in his system.

Recently another 6D model extension of the original Lorenz model was carried out by Howard and Krishnamurthi (1986). They considered a shearing mode as well. Another way of extending the 6D Lorenz system was developed by Humi (2004) and he also showed that the routes to chaos is through the period doubling bifurcation. Another way of constructing generalized Lorenz model was recently studied by Chen and Price (2006). Among the important work in this area Kennamer (1995) constructed 4D, 5D and 6D model respectively. In none of the work reported above the principle of conservation of energy had been considered. The principle was introduced as a mathematical proof for the first time by Theiffault and Horton (1996). They showed that one of the modes in 6D Howard model becomes unbounded in time, that is because the system do not satisfy the principal of conservation of total energy in the dissipationless limit. In this thesis I combine their principle and Saltzman's criterion of selection of

Fourier modes to derive generalized Lorenz systems and also study their routes to chaos. I discovered in that process that in principle there are three methods to construct generalized Lorenz models (1) Method of vertical mode truncation, (2) Method of horizontal mode truncation, (3) Method of both horizontal and vertical mode truncation.

The previous work described above has concerned 2D Rayleigh-Benard convection. However, there are also many published papers dealing with 3D Rayleigh-Benard convection; full reference to theoretical and experimental papers are given by Tong and Gluhovsky (2003) who claimed that with exception of their model and that described by Thieffault (1996) all other models cited by them did not conserve energy in the dissipationless limit. Another model that has not been discussed by Tong is a 9D model of 3D convection developed by Reiterer (1998), who showed that period doubling is the route to chaos in his model. Because of some relevance of this model to my results I will discuss this model in my thesis in later chapters.

1.2 Organization and goals of the thesis

The goals of the thesis are (1) derive generalized Lorenz systems by identifying energy conserving Fourier modes in Saltzman's truncation of the original nonlinear equations describing convection, (2) investigate the routes to chaos in these systems and explain the apparent inconsistency regarding the routes to chaos in previously developed generalized Lorenz systems, (3) show that the system requires higher order modes in order to get coupled with the original Lorenz modes for Method1 but on the

other hand it can get easily coupled to the original Lorenz modes for Method 2, (4) explain quantitatively the difference between these two coupling, (5) demonstrate how to develop high dimensional generalized Lorenz model using this procedure, (6) show that all these systems has bounded solutions.

In Chapter II a generalized Lorenz model is constructed using Method 1and its routes to chaos are investigated and compared with the original Lorenz 3D model. The numerical analysis is based on standard methods used in dynamical systems study such as Fourier power spectra, Lyapunov spectra and phase portraits.

In Chapter III a generalized Lorenz model is derived based on our Method 2 and a short proof is introduced to show how the modes follow a certain rule in order to get coupled with the original Lorenz modes. The routes to chaos are investigated numerically and compared with the routes to chaos obtained in the previous model.

In Chapter IV the final method to derive a generalized Lorenz model is introduced and the energy conserving modes are used to derive yet another generalized Lorenz model and boundedness of solutions is studied. The routes to chaos are investigated using the methods already developed in chapter I and chapter II. This chapter also gives a recipe to add higher order modes to the original model derived by using method III and to construct high dimensional systems.

In Chapter V a full summary of the work is provided including recommended areas for further research and general remarks. The appendices consist of FORTRAN and MATLAB programs that calculate the following: integration of differential

equations, Lyapunov exponents and Fourier power spectral plot. Also it contains the mathematical proof for selection of energy conserving modes and boundedness criterion.

CHAPTER 2

GENERALIZED LORENZ MODEL I

2.1 Vertical mode truncation

A two dimensional and dissipative Rayleigh-Benard convection can be approximated using Lorenz model (1963), which was originally derived by taking into account only three Fourier modes. Numerous attempts have been made to generalize this 3D model to higher dimensions and several different methods of selecting Fourier modes have been proposed. In this chapter generalized Lorenz models with dimension ranging from four to nine are constructed by selecting vertical modes which conserve energy in the dissipationless limit and lead to the systems that have bounded solutions. An interesting result is that lowest order generalized Lorenz model, which satisfies this criteria is a 9D model and that its routes to chaos are the same as that observed in the 3D Lorenz model. Generalized Lorenz system constructed in this chapter are based exclusively on our first method which is stated in the first chapter. The selection of the vertical modes has been done by applying two basic criteria, namely, the conservation of energy in the dissipationless limit and the existence of bounded solutions. I investigate the routes to chaos in these systems and explain the apparent inconsistency in the routes to chaos in the previously developed Lorenz models. My choice of the vertical mode truncation to select the higher order Fourier modes can be physically justified by the fact that the fluid motions in thermal convection are primarily in the

vertical direction and, therefore vertical modes should play dominant role in this description. I will explore generalized Lorenz models constructed using method 2 and 3 in Chapter III and IV respectively.

2.1.1 Derivation of general equations

To describe the method of constructing generalized Lorenz systems, let me consider a 2D model of Rayleigh-Benard convection in a fluid that is treated under Boussinesq approximation and described by the following set of hydrodynamic equations:

$$\frac{\partial V_x}{\partial x}+\frac{\partial V_y}{\partial y}=0,$$
$$\frac{\partial V_x}{\partial t}+V_x\frac{\partial V_x}{\partial x}+V_z\frac{\partial V_x}{\partial z}+(1/\rho)\frac{\partial p}{\partial x}-\nu(\frac{\partial^2 V_x}{\partial x^2}+\frac{\partial^2 V_x}{\partial z^2})=0,$$
$$\frac{\partial V_z}{\partial t}+V_x\frac{\partial V_z}{\partial x}+V_z\frac{\partial V_z}{\partial z}+(1/\rho)\frac{\partial p}{\partial z}-g\alpha T+\nu(\frac{\partial^2 V_z}{\partial x^2}+\frac{\partial^2 V_z}{\partial z^2})=0,$$
$$\frac{\partial T}{\partial t}+V_x\frac{\partial T}{\partial x}+V_z\frac{\partial T}{\partial z}-\kappa(\frac{\partial^2 T}{\partial x^2}+\frac{\partial^2 T}{\partial z^2})=0,$$

where V_x and V_z horizontal and vertical components of the fluid velocity, and the fluid physical parameters are density ρ, pressure p and temperature T. In addition 'g' is gravity, α is the co-efficient of thermal expansion, ν is the kinematic viscosity and κ is the co-efficient of thermal diffusivity.

I assume that the fluid is confined between two horizontal surfaces located at $z=0$ and $z=h$ with $T(z=0)=T_0+\Delta T_0$ and $T(z=h)=T_0$, and that the temperature

varies between surfaces $T(x,z,t) = T_0 + \Delta T_0(1 - z/h) + \theta(x,z,t)$. Using the continuity equation (1.1), we introduce the stream function ψ , which is defined by $V_x = -\frac{\partial \psi}{\partial z}$ and $V_z = \frac{\partial \psi}{\partial x}$. To express the hydrodynamic equations in terms of θ and ψ , we differentiate equation (1.2) and (1.3) with respect to z and x, respectively and subtract former equation from the latter . This gives

$$\frac{\partial}{\partial t}(\nabla^2\psi) - \frac{\partial \psi}{\partial z}\frac{\partial}{\partial x}(\nabla^2\psi) + \frac{\partial \psi}{\partial x}\frac{\partial}{\partial z}(\nabla^2\psi) - g\alpha\frac{\partial \theta}{\partial x} - \nu\nabla^4\psi = 0, \qquad (1.5)$$

Where $\nabla^4 = \frac{\partial}{\partial x^4}^4 + \frac{\partial}{\partial z^4}^4$. The energy equation (1.4) can also be expressed in terms of ψ and θ , and we obtain

$$\frac{\partial \theta}{\partial t} - (\Delta T_0 / h)\frac{\partial \psi}{\partial x} - \frac{\partial \psi}{\partial z}\frac{\partial \theta}{\partial x} + \frac{\partial \psi}{\partial x}\frac{\partial \theta}{\partial z} - \kappa\nabla^2\theta = 0, \qquad (1.6)$$

I follow Saltzman (1962) and introduce the following dimensionless quantities: $x^* = x/h$, $z^* = z/h$, $t^* = t\kappa/h^2$, $\psi^* = \psi/\kappa$, $\theta^* = \theta\alpha g h^3/\kappa\nu$, $\nabla^* = \nabla/h$ .Then equation (1.5) and (1.6) can be written as :

$$\frac{\partial}{\partial t^*}(\nabla^{*2}\psi^*) - \frac{\partial \psi^*}{\partial z^*}\frac{\partial}{\partial x^*}(\nabla^{*2}\psi^*) + \frac{\partial \psi^*}{\partial x^*}\frac{\partial}{\partial z^*}(\nabla^{*2}\psi^*) - \sigma\frac{\partial \theta^*}{\partial x^*} - \sigma\nabla^{*4}\psi^* = 0, \quad (1.7)$$

and

$$\frac{\partial \theta^*}{\partial t^*} - R\frac{\partial \psi^*}{\partial x^*} - \frac{\partial \psi^*}{\partial z^*}\frac{\partial \theta^*}{\partial x^*} + \frac{\partial \psi^*}{\partial x^*}\frac{\partial \theta^*}{\partial z^*} - \kappa\nabla^{*2}\theta^* = 0, \qquad (1.8)$$

where $\sigma = \nu / \kappa$ is the Prandtl number and $R = \alpha g h^3 \Delta T_0 / \nu\kappa$ is the Rayleigh number. I refer to these set of equations as Saltzman's equations. According to Saltzman one may impose the following boundary conditions: $\psi^* = 0$, $\nabla^{*2}\psi^* = 0$ and $\theta^* = 0$ at both surfaces $z = 0$ and $z = h$, and write the double Fourier expansions ψ^* and θ^*

$$\psi(x^*, z^*, t^*) = \sum_{m=-\infty}^{\infty} \sum_{n=-\infty}^{\infty} \psi(m, n, t^*) \exp(2\pi i h((m/L)x^* + (n/2h)z^*) \qquad (1.9)$$

$$\theta(x^*, z^*, t^*) = \sum_{m=-\infty}^{\infty} \sum_{n=-\infty}^{\infty} \theta(m, n, t^*) \exp(2\pi i h((m/L)x^* + (n/2h)z^*) \qquad (1.10)$$

where L is the characteristic scale representing periodicity $2L$ in the horizontal direction. Saltzman (1962) expressed ψ and θ in terms of their real and imaginary parts, $\psi(m,n) = \psi_1(m,n) - i\psi_2(m,n)$ and $\theta(m,n) = \theta_1(m,n) - i\theta_2(m,n)$, which do not show explicit time-dependence, substituted the above solutions to equations (1.7) and (1.8). The general result was a set of first order differential equations for the Fourier coefficients ψ_1, ψ_2, θ_1 and θ_2 . However, when the theory is applied to describe the cellular convective motions originating from small perturbations, Saltzman fixed the vertical nodal surfaces of the convection cell by excluding all $\psi_2(m,n)$ and $\theta_1(m,n)$ modes .This Saltzman rule is used by Lorenz in his derivation of a 3D system (1963) and I will also use the same rule in my construction of higher dimensional Lorenz models. In addition both Lorenz and Saltzman did not consider shear flows by

excluding the ψ_1 modes with $m = 0$, so the same assumption would hold in my derivation.

2.1.2 From 3D to 6D Lorenz model

Lorenz[1] selected the following three Fourier modes: $\psi_1(1,1)$, which describes the circular convection of roll, and $\theta_2(1,1)$ and $\theta_2(0,2)$, which approximates the vertical and horizontal temperature differences in the convective roll., respectively. He introduced the new variables $X(t) = \psi_1(1,1)$, $Y(t) = \theta_2(1,1)$, $Z(t) = \theta_2(0,2)$ and derived the following three ordinary nonlinear differential equations approximating nonlinear convection in time.

$$\frac{dX}{d\tau} = \sigma(Y - X) \tag{1.11}$$

$$\frac{dY}{d\tau} = rX - Y - XZ \tag{1.12}$$

$$\frac{dZ}{d\tau} = XY - bZ \tag{1.13}$$

Where $r = R / R_c$, $\tau = \pi^2(1 + a^2)t^*$ is the dimensionless time, $a = h / L$ is the aspect ratio and $b = 4/(1 + a^2)$. The modes selected by Lorenz while truncating the original nonlinear equations are such that the 3D dynamical system conserves energy in the dissipation less limit (J.H.Curry(1978)). In addition the solution of the Lorenz equations are bounded.

To extend the 3D Lorenz model to higher dimensions, one must select higher order Fourier modes. As already discussed there are three different ways of selecting higher order modes. In this chapter I construct a high dimensional extension based on method 1, which is basically vertical mode truncation, which means we fix the value of m by taking m = 1 and add the vertical modes in both the stream function and temperature variations (see equation 1.9 and 1.10) . Following this procedure we select the $X_1 = \psi_1(1,2)$, $Y_1 = \Theta_2(1,2)$ and $Z_1 = \Theta_2(0,4)$ the fact that the later mode has to be considered along with the two former modes has been demonstrated by Thieffault and Horton(1996) based on the energy conserving principle. Hence, I introduce X_1, Y_1, Z_1 and obtain the following set of equations:

$$\frac{dX}{d\tau} = -\sigma X + \sigma Y \tag{1.14}$$

$$\frac{dY}{d\tau} = -XZ + rX - Y \tag{1.15}$$

$$\frac{dZ}{d\tau} = XY - bZ \tag{1.16}$$

$$\frac{dX_1}{d\tau} = -\sigma c_1 X_1 + \frac{\sigma}{c_1} Y_1 \tag{1.17}$$

$$\frac{dY_1}{d\tau} = rX_1 - c_1 Y_1 - 2X_1 Z_1 \tag{1.18}$$

$$\frac{dZ_1}{d\tau} = 2X_1 Y_1 - 4bZ_1 \tag{1.19}$$

Since the original Lorenz variables (X, Y, Z) are decoupled from the new variables (X_1, Y_1, Z_1), the obtained set of equations therefore do not describe a 6D system but instead two independent systems. One may attempt to construct a 5D system by taking $\theta_2(0,2) = 0$ and a 4D model with $\theta_2(1,2) = \theta_2(0,2) = 0$, but in both cases the additional equations are not coupled to the original Lorenz equations.

2.1.3 From 6D to 9D Lorenz model

Since the model derived in the previous section do not form a new system therefore I keep adding modes to determine the lowest order generalized Lorenz model. Using the vertical mode truncations, we select the $X_2 = \psi_1(1,3)$, $Y_2 = \theta_2(1,3)$ and $Z_2 = \theta_2(0,6)$ modes and derive the following set of first order differential equations:

$$\frac{dX}{d\tau} = -\sigma X + \sigma Y \tag{1.20}$$

$$\frac{dY}{d\tau} = -XZ + rX - Y + ZX_2 - 2X_2Z_1 \tag{1.21}$$

$$\frac{dZ}{d\tau} = XY - bZ - X_2Y - XY_2 \tag{1.22}$$

$$\frac{dX_1}{d\tau} = -\sigma c_1 X_1 + \frac{\sigma}{c_1} Y_1 \tag{1.23}$$

$$\frac{dY_1}{d\tau} = -2X_1Z_1 + rX_1 - c_1Y_1 \tag{1.24}$$

$$\frac{dZ_1}{d\tau} = 2XY_2 + 2YX_2 + 2X_1Y_1 - 4bZ_1 \tag{1.25}$$

$$\frac{dX_2}{d\tau} = -\sigma c_2 X_2 + \frac{\sigma}{c_2} Y_2 \tag{1.26}$$

$$\frac{dY_2}{d\tau} = XZ + rX_2 - c_2 Y_2 - 2XZ_1 - 3X_2 Z_2 \tag{1.27}$$

$$\frac{dZ_2}{d\tau} = 3X_2 Y_2 - 9bZ_2 \tag{1.28}$$

It is seen that the derived 9D system the modes given by the variables X_1, $X_2, Y_1, Y_2,$ Z_1 and Z_2 are coupled to the original Lorenz modes X, Y and Z, which means this is a generalized Lorenz model. In order to determine whether this is lowest order generalized Lorenz model, I must now consider 8D and 7D systems which are the subset of this 9D model. To obtain the 8D system, I assume that $Z_2 = 0$ and use it to reduce the above set of equations. The last term in equation (1.27) as a result becomes zero and in addition (1.28) yields the condition $X_2 Y_2 = 0$, which clearly indicates 8D is too limited to represent a new generalized system. Even more severe restriction occur when 7D system is derived by taking into account $Y_2 = 0$. Since neither 8D or7D forms a new system, I conclude that the 9D model described by (1.20) to (1.28) is indeed the lowest order generalized Lorenz system that can be obtained by the method of vertical mode truncation. Now it remains to be checked whether my new 9D model conserves energy in the dissipation less limit and has bounded solutions.

2.1.4 Validity criteria

There are two validity criteria that our new 9D system must satisfy in order to be considered a physically meaningful system. The first criteria requires that the energy is conserved in the dissipation less limit; from now on when I refer to the conservation of energy I would always mean it's conservation in the dissipation less limit. The fact that some higher dimensional models of Rayleigh-Benard convection do not conserve energy in the dissipation less limit has already been recognized in literature (Theiffault (1996), Tong (2003)). There are many reasons for having energy conserving generalized Lorenz systems. Among these reasons let me explain a few: (1) the effects of non conservation of energy could be large and they are relevant to the energy flow in the dissipative regime, (2) the thermal flux in the steady-state is correctly described only by energy conserving systems, (3) energy conserving truncations represents the whole system more accurately and they reduce unphysical numerical instabilities. The second requirement for this system is to have bounded solutions; systems with unbounded solutions are treated as unphysical. This criterion has been used by many authors to validate their generalized Lorenz systems.

According to Saltzman (1962), the dimensionless kinetic, K^*, and potential , U^*, can be expanded into spectral components as

$$K^* = \frac{1}{2}\sum_{m=-\infty}^{\infty}\sum_{n=-\infty}^{\infty}\delta^2(m,n)\left|\psi(m,n)\right|^2 \tag{1.29}$$

$$U^* = -\frac{1}{2}\frac{\sigma}{R}\sum_{m=-\infty}^{\infty}\sum_{n=-\infty}^{\infty}\left|\Theta(m,n)\right|^2 \tag{1.30}$$

where $\delta^2(m,n) = \left\{(2\pi a)^2 m^2 + \pi^2 n^2\right\}$.

I now apply these formulas to our 9D model to obtain

$$K^* = \frac{1}{2}[\delta^2(1,1)X^2 + \delta^2(1,2)X_1^{\,2} + \delta^2(1,3)X_2^{\,2}] \tag{1.31}$$

$$U^* = -\frac{1}{2}\frac{\sigma}{R}(Y^2 + Y_1^2 + Y_2^{\,2} + Z^2 + Z_1^{\,2} + Z_2^{\,2}) \tag{1.32}$$

where $\delta^2(1,1), \delta^2(1,2), \delta^2(1,3)$ are constants. To verify that the total energy $E^* = K^* + U^*$, is conserved I write equation (1.30) as follows:

$$\frac{dE^*}{d\tau} = -\sigma[\delta^2(1,1)(X-Y) + \delta^2(1,2)(c_1X_1 - \frac{1}{c_1}Y_1) + \delta^2(1,3)(c_2X_2 - \frac{1}{c_2}Y_2)] - \frac{\sigma}{R}(\dot{Y} + \dot{Y}_1 + \dot{Y}_2 + \dot{Z} + \dot{Z}_1 + \dot{Z}_2)$$

using equation (1.20), (1.23) and (1.26) in the dissipation less limit

When $\sigma \to 0$ equation (1.33) becomes

$$\lim_{\sigma\to 0}\frac{dE^*}{d\tau} = 0, \tag{1.33}$$

which gives $E^* = K^* + U^*$ is constant. Hence the 9D system conserves energy in the dissipation less limit. To show that this 9D system has bounded solutions I introduce a quantity called Q (see Appendix A) defined as

$$Q^* = K^* + 2\sum_{i=1}^{3}|Y_i|^2 + \sum_{j=1}^{3}(Z_j - \frac{2}{n})^2 \tag{1.34}$$

Note that all selected modes are included in Q, so if one of them diverges, then Q would also diverge. To obtain the condition for bounded solutions, we take the time derivative of Q and write

$$\frac{dQ^*}{d\tau} \leq [-\min(2\nu, \kappa)Q + 4\kappa n_0] \tag{1.35}$$

where n_0 is the number of Z modes. To have $\frac{dQ^*}{d\tau} < 0$, one must have $Q > 4\kappa n_0 / \min(2\nu, \kappa)$, which is the condition for bounded solutions. This condition was checked numerically for the 9D system and found to be always satisfied. Hence the conclusion the model has bounded solutions.

2.1.5 Comparison with previous works

The most important previous work has already been described in the introduction in Chapter I and as well as in section 1 of chapter II. Here, I make a comparison between my results and those obtained by Kennamer (1995), Humi (2004), Curry (1978) and Reiterer (1998). The main reason for this selective comparison is that only generalized Lorenz systems constructed by these authors are directly relevant to our models. Since in all these cases higher-order modes were added to the original three modes picked up by Lorenz, in the following, I only list those extra modes.

An interesting result has been found by Kennamer (1995) who selected the $\psi_1(1,3)$, $\theta_2(1,3)$ and $\theta_2(0,4)$ modes and obtained an extension of Lorenz model in six dimensions. He showed that his three extra modes are coupled to the original Lorenz modes.(see section 2.4) and that the solutions to these equations were bounded. The result presented in Appendix B also shows that this model does conserves energy. Comparison of this 6D model with my uncoupled 6D model given by equations (11) –

(16) clearly shows that Kennamer omitted the modes $\psi_1(1,2)$ and $\theta_2(1,2)$ without giving any physical justifications. In addition his selection of $\theta_2(0,4)$ seems to be inconsistent with a general principle of selecting modes as formulated by Theiffault and Horton (1996).

Another 6D Lorenz model was constructed by Humi [10] who selected $\psi_1(1,2)$, $\psi_1(2,1)$ and $\theta_2(1,2)$ modes and showed that the solutions were bounded. Comparison with our uncoupled 6D system shows that the $\theta_2(0,4)$ mode in my model was replaced by the $\psi_1(2,1)$ mode. This replacement is not consistent with Theiffault and Horton's principle and therefore it does not conserve total energy. The latter is easy to demonstrate by using the results given in section (2.1.3).

A generalized model developed by Curry (1978) has 14 dimensions and it was constructed by using six ψ_1 modes and six θ_2 modes with $1 \le m \le 3$ and $1 \le n \le 4$, in addition the $\theta_2(0,2)$ and $\theta_2(0,6)$ modes. Curry demonstrated that his 14D model had bounded solutions, however he did not check the conservation of energy. The results of section (2.1.3) can be used to show that the system does not conserves energy. Note that the 6D model constructed by Kennamer [6] is a subset of this 14D model but Humi's 6D model or the 9D model are the subset of Curry's general system.

Finally I want to compare the 9D Lorenz system derived in section 2.1.2 to that developed by Reiterer et al. (1998). To describe 3D square convection cells , the authors have expanded the x, y, z components of a vector potential A, with $\vec{V} = \nabla \times \vec{A}$, and

the temperature variations θ into triple Fourier series, with l, m, n representing the modes in the y, x and z direction(see equations 1.9 and 1.10) , respectively. These Fourier expansions have been truncated up to second order and a 9D Lorenz system was derived. The authors strongly emphasized that they used a mathematically consistent approach to select the modes and that all second-order modes have been included in the derivation. The model is presented in this chapter section 2.5, where we also show that

This mathematically consistent approach leads to a 9D system that violates the principle of conservation of energy.

2.1.6 Routes to chaos

After demonstrating that my 9D system conserves energy in the dissipation less limit and has bounded solutions, I may now investigate the onset of chaos in this system and determine the routes to chaos. To achieve this, I solved numerically the set of equations (1.17) through (1.25) by fixing parameters $b = 8/3$ and $\sigma = 10$, and varying the control parameter over the range $0 \le r \le 50$. The main purpose of this calculation was to determine the value of r for which fully developed chaos is observed and to determine route that lead to the chaotic regime. The obtained results are presented by using phase portraits, power spectra and Lyapunov spectra.

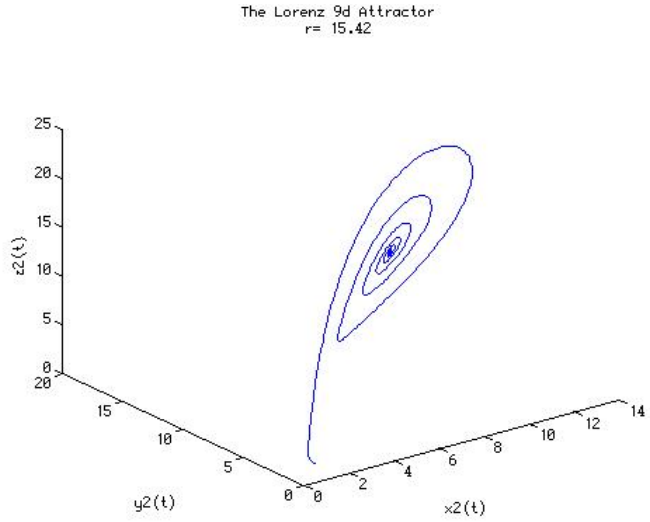

2.1 Phase space portrait of x, y, z at r =15.42

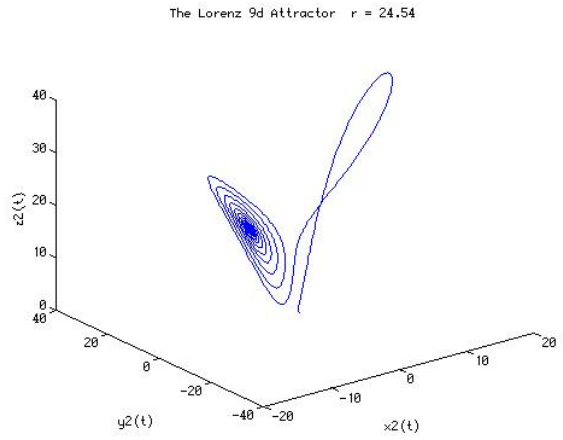

2.2 Phase space portrait of x, y, z at r =24.54

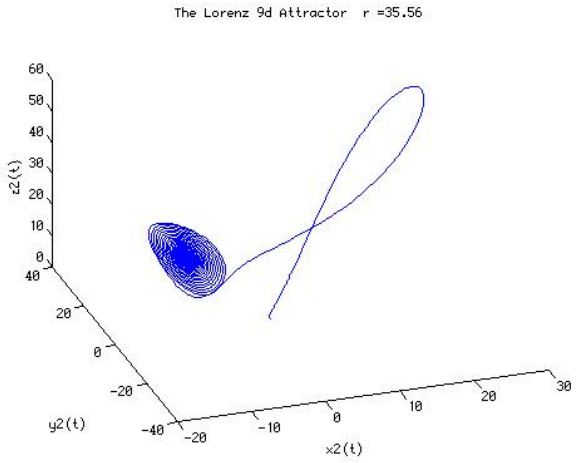

2.3 Phase space portrait of x, y, z at r =35.56

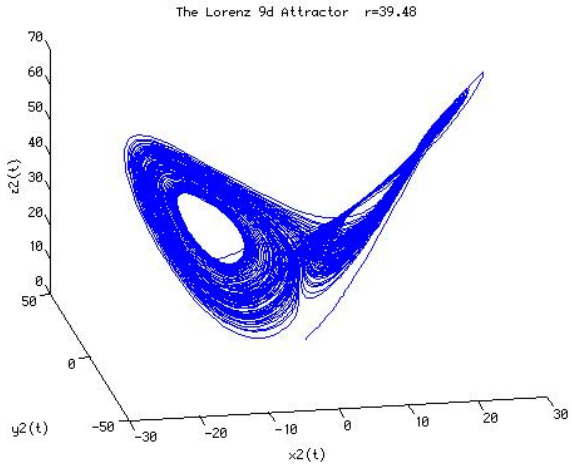

2.4 Phase space portrait of x, y, z at r =39.48

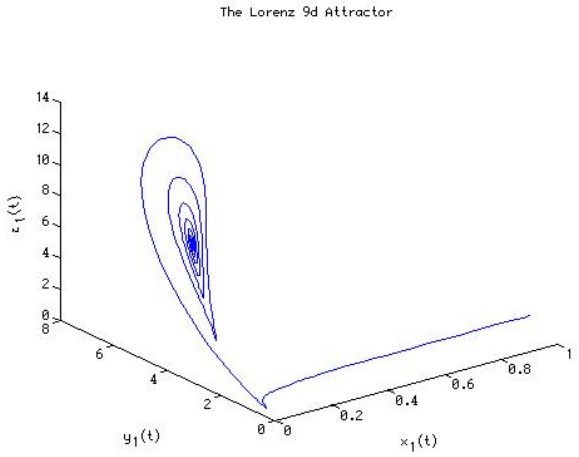

2.5 Phase space plot of Lorenz 9D at r =18.42

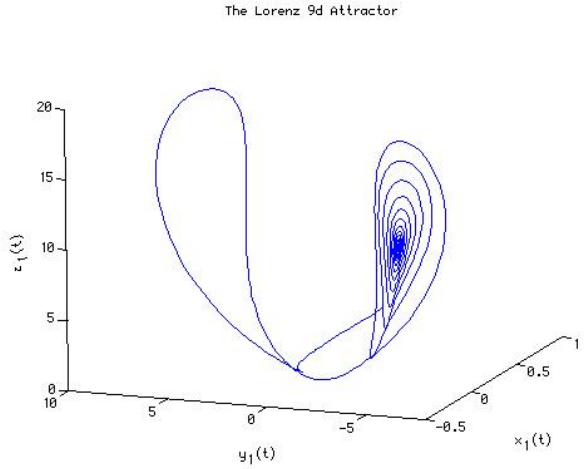

2.6 Phase space plot of Lorenz 9D at r =24.54

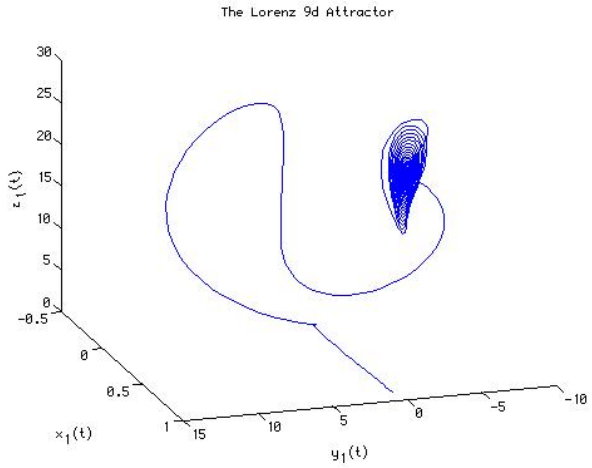

2.7 Phase space plot of Lorenz 9D at r =34.54

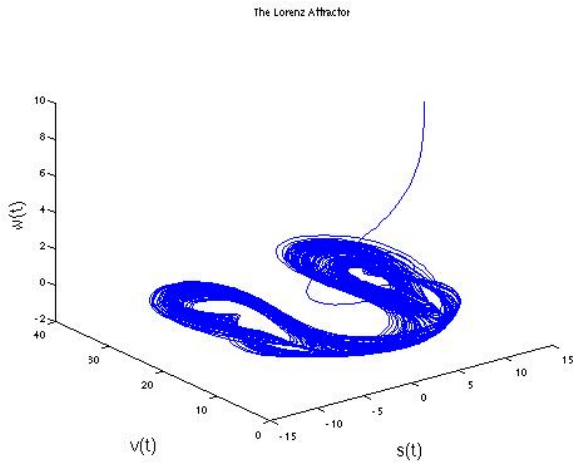

2.8 Phase space plot of Lorenz 9D at r =42.48

The phase portrait for the set of variables (X, Y, Z) and (X_1, Y_1, Z_1) are given in Figures 2.1 through 2.8.The result presented in these figures show time evolution of the system from given initial conditions to a periodic or strange attractor. The panels of Figs 1 and 3 clearly show periodic behavior of the system for the values of r ranging from 24 to 34. Periodic behavior is also seen in the upper panel of Figs 2 and 4, where phase portraits for $r = 40$ are presented. Prominent chaotic behavior of the system is seen in the lower panels of Figures 2.4 and 2.8, where system's strange attractor is displayed for $r = 42.12$. The strange attractor has the same properties as the Lorenz strange attractor, these properties are either best displayed in (X, Y, Z) or (X_1, Y_1, Z_1) variables. Changes in the behavior of the system with the increasing value of r are also seen in the Figures 2.10-2.14, which presents the power spectra. The broad band power spectrum shown in the lower panel of Fig.2.14 represents additional strong evidence that the system has entered fully developed chaotic regime.

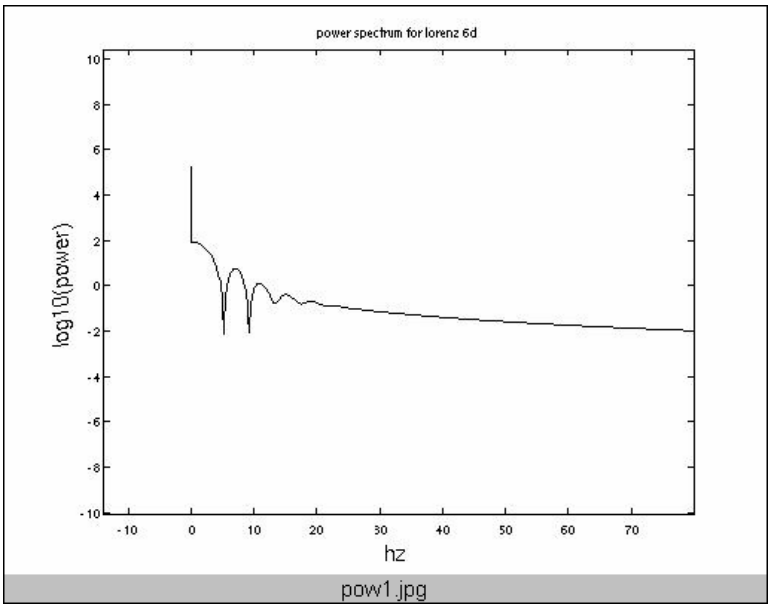

2.9 Power spectrum for Lorenz 9D at r =15.42

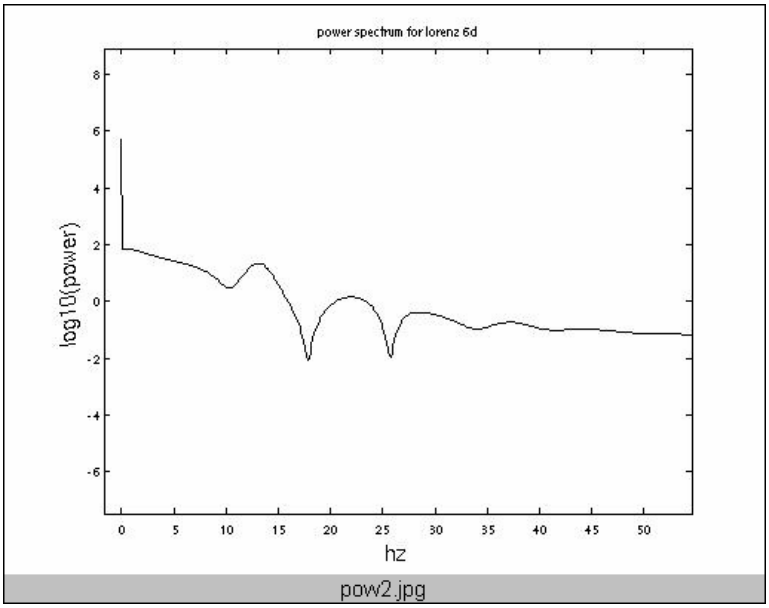

2.10 Power spectrum for Lorenz 9D at r =20.54

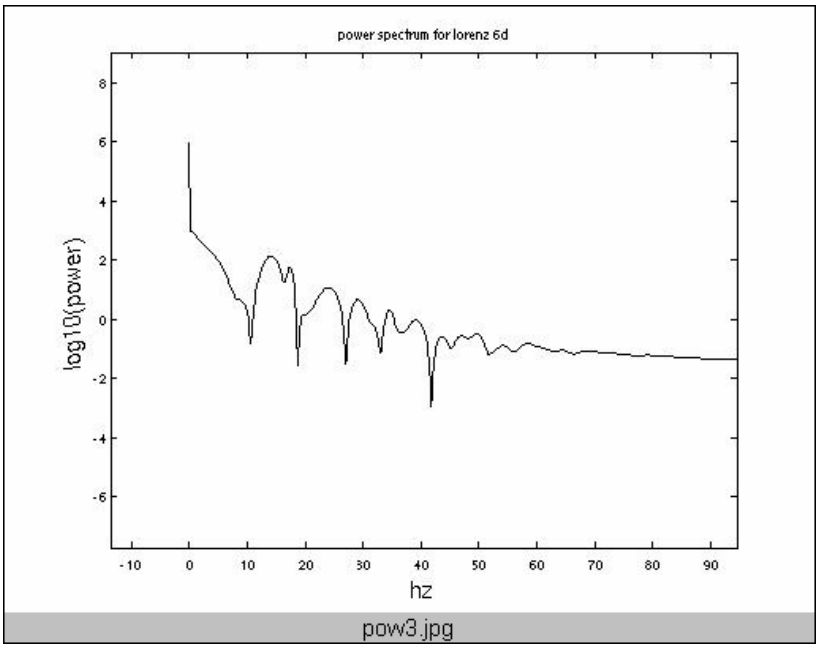

2.11 Power spectrum for Lorenz 9D at r =24.54

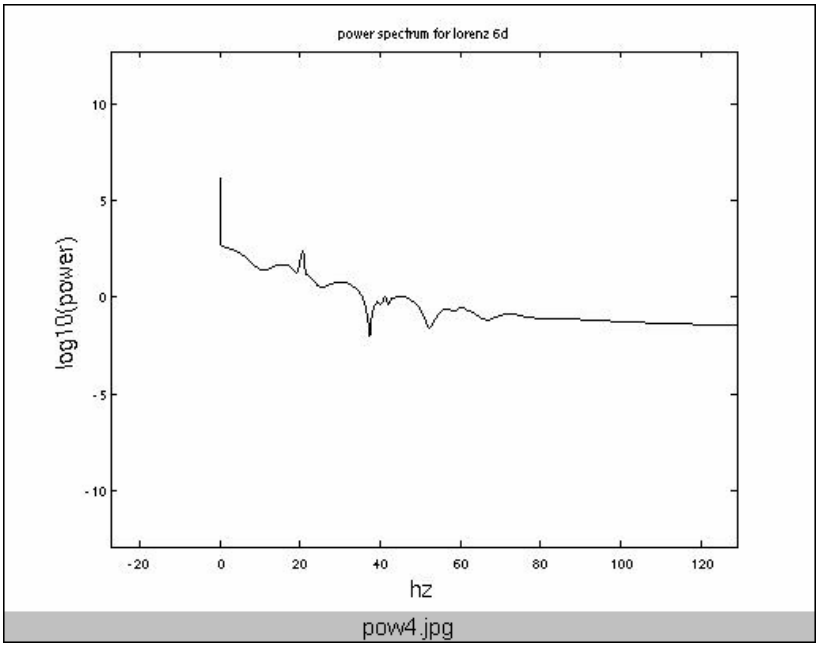

2.12 Power spectrum for Lorenz 9D at r =28.54

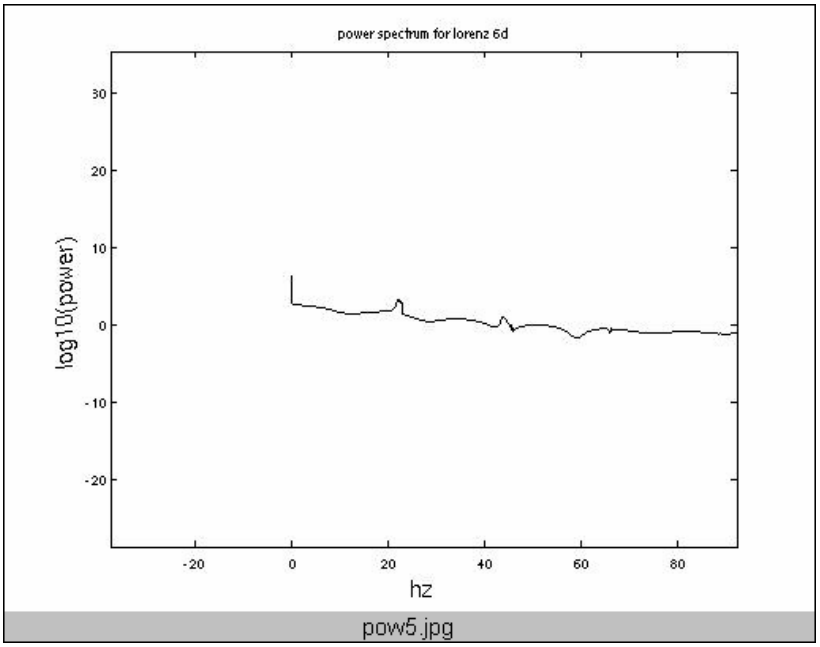

2.13 Power spectrum for Lorenz 9D at r =38.54

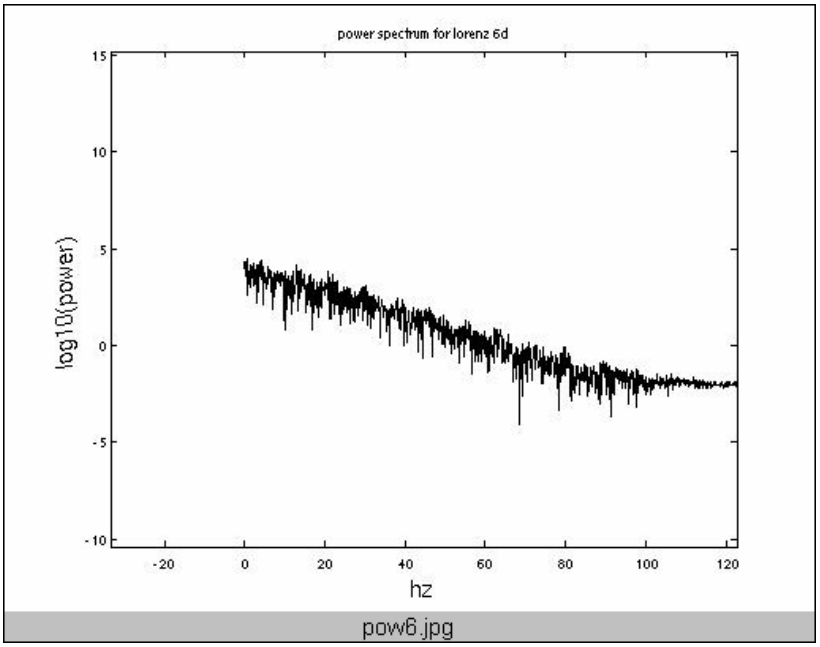

2.14 Power spectrum for Lorenz 9D at r =42.54

To determine the route to chaos of this system and the precise value of r at which the system enters the chaotic regime, we calculated all nine Lyapunov exponents for the system. The three leading Lyapunov exponents are plotted versus r in Fig.2.15. The plots show that one Lyapunov exponent becomes positive when $r = 40.43$, however further increase of r leads to several spikes that quickly disappear at $r = 40.49$. The same Lyapunov exponent become positive again at $r = 41.10$ and it shows many spikes that implies that the system is entering full chaos via chaotic transients, which is the same route that observed in the original Lorenz 3D system. After the last negative spike at $r = 41.44$, fully developed chaos is observed when $r \geq 41.54$. These results are consistent with those shown in Figs 2.1 through 2.8.

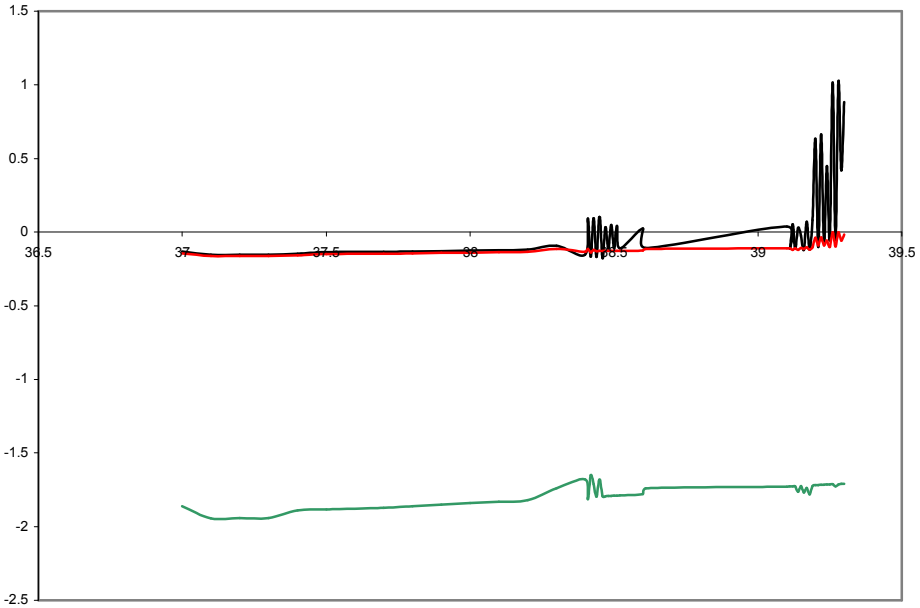

2.15 Three leading Lyapunov exponents for Lorenz 9D

There are similarities between my result obtained for the 9D system and the original 3D Lorenz model(1963), and the 6D model constructed by Kennamer (1995); note that all three models are energy conserving systems. Both the 9D and 6D systems have strange attractors that are very similar to the Lorenz strange attractor. In addition, the route to chaos via chaotic transients observed in the 9D and 6D system is the same as that identified for the 3D Lorenz system (1963). The only important difference between these three models is that each one of them exhibits fully developed chaos for a different value of parameter r. For the 3D system, this critical value of r=24.75, for the 6D system it is $r = 40.15$, and finally for my 9D system $r = 41.54$ is required. This implies the larger the number of Fourier modes taken into account the higher the value of r required for the system to enter the fully developed chaotic regime.

It now becomes clear that the period-doubling route to chaos discovered by Humi (2004) and Reiterer (1998) in their generalized Lorenz models was caused by their selection of the modes that do not conserve energy. The same is true for the 14D system constructed by Curry (1978) as this system also violates the principle of conservation of energy. My results show that the energy conserving generalized Lorenz models have the same routes to chaos as the original 3D Lorenz model, which is a subset of these models.

2.1.7 Another 6D Lorenz model

Kennamer (1995) constructed a new 6D Lorenz system by selecting $X1(t) = \psi_1(1,3)$, Y1(t) =$\Theta_2(1, 3)$ and Z1(t) = $\Theta_2(0, 4)$ in addition to the three modes originally chosen by Lorenz (1963).

The 6D system is described by the following set of nonlinear and first-order differential equations:

$$\frac{dX}{d\tau} = -\sigma X + \sigma Y \tag{1.34}$$

$$\frac{dY}{d\tau} = -XZ+rX-Y+ZX_1 -2X_1Z_1 \tag{1.35}$$

$$\frac{dZ}{d\tau} = XY - bZ - XY_1 - X_1Y \tag{1.36}$$

$$\frac{dX_1}{d\tau} = -c_1\sigma X_1 + \frac{\sigma}{c_1} Y_1 \tag{1.37}$$

$$\frac{dY_1}{d\tau} = XZ - 2XZ_1 + rX_1 - c_1Y_1 \tag{1.38}$$

$$\frac{dZ_1}{d\tau} = 2XY_1 + 2YX_1 - 4bZ_1 \tag{1.39}$$

where $\tau = \pi^2(1+a^2)t^*$ is the dimensionless time, a = h/L is the aspect ratio, b = $4/(1+a^2)$, r = R/R_c with $R_c = \pi^4(1+a^2)^3/a^2$ and c_1 = $(9+a^2)/(1+a^2)$. Kennamer already demonstrated that this system has bounded solutions and its route to chaos is via chaotic transients (1995). We now show that the system conserves energy in the

dissipationless limit. Based on the results obtained in Sec. II.D., we know that the potential energy U^* approaches zero as $\sigma \to 0$, thus, we only calculate the kinetic energy K^* of the system and obtain

$$K^* = \frac{1}{2}[\delta^2(1,1)X^2 + \delta^2(1,3)X_1^{\,2}] \tag{1.40}$$

where $\delta^2(1,1)$ and $\delta^2(1,3)$ are constants. The time derivative of K^* is

$$\frac{dK^*}{d\tau} = \delta^2(1,1)\dot{X} + \delta^2(1,3)\dot{X}_1 \tag{1.41}$$

We replace $\dot{X}$ and $\dot{X}_1$ by the RHS of Equations (1.34) and (1.37), respectively, and take the limit of $\sigma \to 0$. Then, we have

$$\lim_{\sigma \to 0} \frac{dE^*}{d\tau} = 0 \tag{1.42}$$

Which gives $E^* = K^* + U^*$ = const and shows that the total energy of this 6D system is conserved.

2.1.8 Another 9D Lorenz model

A system that is of special interest here is a 9D model developed by Reiterer (1998). To describe 3D square convection cells, the authors have expanded the x, y and z components of a vector potential A, with V = r × A, and the temperature variations θ into triple Fourier expansions, with l, m and n representing the modes in the y, x and z direction (see Equations (1.9) and (1.10)), respectively. These Fourier expansions have been truncated up to the second order and the following Fourier modes have been used: X(t) = A1(0, 2, 2), X1(t) =A1(1, 1, 1), X2(t) = A2(2, 0, 2), Y (t) = A2(1, 1, 1), Y1(t) =

A3(2, 2, 0), Y2(t) = Θ (0, 0, 2), Z(t) = Θ (0, 2, 2), Z1(t) = Θ (2, 0, 2) and Z2(t) = Θ (1, 1, 1), where A1, A2, A3 and Θ are the Fourier coefficients of the Ax, Ay, Az and θ expansions, respectively. This selection of Fourier modes leads to the following equations:

$$\frac{dX}{d\tau} = -\sigma b_1 X - X_1 Y + b_4 Y^2 + b_3 X_2 Y_1 - \sigma b_2 Z \tag{1.43}$$

$$\frac{dX_1}{d\tau} = -\sigma X_1 + XY - X_1 Y_1 + YY_1 - \frac{1}{2}\sigma Z_2 \tag{1.44}$$

$$\frac{dX_2}{d\tau} = -\sigma b_1 X_2 + X_1 Y - b_4 X_1^{\,2} - b_3 XY_1 + \sigma b_2 Z_1 \tag{1.45}$$

$$\frac{dY}{d\tau} = -\sigma Y - X_1 X_2 - X_1 Y_1 + YY_1 + \frac{1}{2}\sigma Z_2 \tag{1.46}$$

$$\frac{dY_1}{d\tau} = -\sigma b_5 Y_1 + \frac{1}{2}X^2 - \frac{1}{2}Y^2 \tag{1.47}$$

$$\frac{dY_2}{d\tau} = -b_6 Y_2 + X_1 Z_2 - YZ_2 \tag{1.48}$$

$$\frac{dZ}{d\tau} = -b_1 Z - rX + 2Y_1 Z_1 - YZ_2 \tag{1.49}$$

$$\frac{dZ_1}{d\tau} = -b_1 Z_1 + rX^2 - 2Y_1 Z + X_1 Z_2 \tag{1.50}$$

$$\frac{dZ_2}{d\tau} = -Z_2 - rX_1 + rY - 2X_1 Y_2 + 2YY_2 + YZ - X_1 Z_1 \tag{1.51}$$

where $\tau = (1 + 2\kappa^2)$t, with $\kappa = \kappa_x = \kappa_y$, b1 = $4(1 + \kappa^2)/(1 + 2\kappa^2)$, b2 = $(1 + \kappa^2)/2(1 + \kappa^2)$, b3 = $2(1-\kappa^2)/(1+ \kappa^2)$, b4 = k2/$(1 +\kappa^2)$, b5 = $8\kappa^2/(1 + 2\kappa^2)$ and b6 = $4/(1 + 2\kappa^2)$.

Detailed numerical studies of this 9D system have been done by Reiterer et al. (1998), who showed that the system had bounded solutions and its route to chaos was via period-doubling. Comparison of this set of equations to that given in Sec. II (see Equations 1.20 through 1.28) shows that these two 9D models are completely different. One obvious reason for this difference is the fact that my 9D model and their 9D models describe 2D and 3D Rayleigh-B´enard convection, respectively. Another more important reason for the difference is that my 9D model does conserve energy in the dissipation less limit, however, their 9D model does not. To demonstrate this, we use Equations (26) and (27), and extend them by adding summation over l. Since the potential energy approaches zero as $\sigma \to 0$, we only calculate the kinetic energy of the system and obtain

$$K = \frac{1}{2}[c_1 X^2{}_1 + c_2 X_1^2 + c_3 X_2{}^2 + c_4 Y^2 + c_5 Y_1^2] \tag{1.52}$$

where c_1, c_2, c_3, c_4 and c_5 are constants that depend on l, m and n (see Equations. (26)). Taking derivative with respected to time, we get

$$\frac{dK}{d\tau} = c_1\dot{X} + c_2\dot{X}_1 + c_3\dot{X}_2 + c_4\dot{Y} + c_5\dot{Y}_1 \tag{1.53}$$

and use Equations (1.44) through (1.48) to calculate the time derivatives of X, X1, X2, Y and Y1. Since there are several terms on the RHS of Equations (44) - (48) that do not explicitly depend on σ, those terms will remain non-zero when the limit $\sigma \to 0$ is applied to Equation. (1.53). Hence, I obtain

$$\lim_{\sigma \to 0} \frac{dE}{d\tau} \neq 0 \qquad (1.54)$$

Where E = K + U. This shows that the total energy of the 9D system constructed by Reiterer (1998) is not conserved and, therefore, their results on the onset of chaos and route to chaos in this system are not valid. The energy conserving 9D Lorenz model for a 2D Rayleigh-B´enard convection is presented in Sec. II of this thesis.

CHAPTER 3

GENERALIZED LORENZ MODEL II

3.1 Horizontal mode truncations

3.1.1 Introduction

All attempts to generalize the three dimensional Lorenz model by selecting higher order Fourier modes can be divided into three categories, namely: vertical, horizontal and vertical-horizontal mode truncations. The previous chapter showed that the first method allowed only construction of at least a 9D system when the selected modes were energy conserving. The results presented in this chapter demonstrate that a 5D model is the lowest-order generalized Lorenz model that can be constructed by the second method and that its route to chaos is the same as that observed in the original Lorenz model. It is shown that the onset of chaos in both systems is determined by a number of modes that determines the vertical temperature difference in a convection roll, which make sense because after all in this simplified model of convection the main driving force of the system is the vertical temperature difference. In addition, a simple yet general rule is proposed that allows selecting modes that conserves energy for each method.

3.1.2 Derivation of 5D Lorenz model

In order to derive lowest order generalized Lorenz model using horizontal mode truncations I would use the equations (1.9) and (1.10) already derived in Chapter 1.The boundary condition is the same as stated in the Saltzman derivation. As already stated Fourier mode $\psi_1(1,1)$, that describes the circulation of convection roll and $\theta_2(1,1)$ and $\theta_2(0,2)$ which describe the horizontal and vertical temperature difference in the convective roll were selected by Lorenz to construct his 3D model. Here I select higher order Fourier modes by using the method of horizontal mode truncations. The original 3D Lorenz model is treated as the basis and the higher modes are added until the lowest order generalized Lorenz model is obtained. I begin with two Fourier modes $\psi_1(2,1)$ and $\theta_2(2,1)$, and find that they are already coupled to the original Lorenz modes. The coupling is shown by a resulting set of ordinary differential equations:

$$\frac{dX}{d\tau} = -\sigma X + \sigma Y \tag{3.1}$$

$$\frac{dY}{d\tau} = rX - XZ - Y \tag{3.2}$$

$$\frac{dZ}{d\tau} = XY - bZ + 2X_1Y_1 \tag{3.3}$$

$$\frac{dX_1}{d\tau} = -c_1\sigma X_1 + (\sigma / c_1)2Y_1 \tag{3.4}$$

$$\frac{dY_1}{d\tau} = -2X_1Z + 2rX_1 - c_1Y_1 \tag{3.5}$$

Since coupling already takes place in this 5D model I conclude that this is the lowest-order generalized model that can be constructed by using the horizontal mode truncations. As expected the model reduces to the 3D Lorenz model when $X_1 = Y_1 = 0$. Now I can use the method presented in Chapter II to show that this generalized Lorenz model also conserves energy in the dissipationless limit and has bounded solutions. As a result we call the $X_1 = \psi_1(2,1)$ and $Y_1 = \theta_2(2,1)$ the energy-conserving modes.

3.2 Coupling of modes via a simple rule

An interesting result which I discovered seems to mediate a general coupling of higher modes to original Lorenz modes while deriving generalized Lorenz model. This was not apparent until I derived the 5D model using horizontal mode truncations. An interesting result is that horizontal and vertical mode truncation lead to systems having different dimensions. This clearly indicates that the vertical and the horizontal modes are coupled to original Lorenz modes quite differently. The main problem to be recognized is whether a mode is coupled or not, and identify a rule which underlies this coupling. In the following both issues are discussed in detail. As already mentioned in the previous chapter while deriving the basic equations, Saltzman expressed the coefficients $\psi(m,n)$ and $\theta(m,n)$ see equation (3.1) and (3.2) in terms of their real and imaginary parts and applied such boundary conditions that that all the modes $\psi_2(m,n), \theta_1(m,n)$ and $\psi_1(0,n)$ are excluded. He derived the following set of first order differential equations:

$$\frac{d\psi_1}{dt^*} = \sum_{p=-\infty}^{\infty} \sum_{q=-\infty}^{\infty} C(m,n,p,q) \frac{\beta^2(p,q)}{\beta^2(m,n)} \psi_1(p,q)\psi_1(m-p,n-q) - \frac{\sigma l^* m}{\beta^2(m,n)} \theta_2(m,n) - \alpha\beta^2(m,n)\psi_1(m,n)$$

$$\frac{d\theta_2}{dt^*} = -\sum_{p=-\infty}^{\infty} \sum_{q=-\infty}^{\infty} C(m,n,p,q)\psi_1(p,q)\theta_2(m-p,n-q) - Rl^* m\psi_1(m,n) - \beta^2(m,n)\theta_2(m,n)$$

where $t^* = t\kappa / h^2$ is dimensionless time, $\beta^2(m,n) = l^{*2}m^2 + \pi^2 n^2$ and $\sigma = \nu / \kappa$ is the Prandtl number, with ν and κ being the kinematic viscosity and the coefficient of thermal diffusivity, respectively. In addition, $l^* = 2\pi h / L$ and $R = \alpha g h^3 \Delta T_0 / \kappa\nu$ is the Rayleigh number, with α being constant of thermal expansion, g being gravity, and ΔT_0 representing vertical temperature difference in the convective region.

Using the above equations, it is easy to determine whether a selected mode is coupled to the original Lorenz system or not. As an example, let me consider the vertical mode $\psi_1(1,2)$. Since m=1, n=2, equation (1.8) shows there is no way to couple this mode to $\psi_1(1,1)$. In addition equation (1.9) shows that $\psi_1(1,2)$ can neither be coupled to $\theta_2(1,1)$ nor to $\theta_2(0,2)$.Let us now consider the horizontal modes $\psi_1(2,1)$ and $\theta_2(2,1)$. Clearly these modes still can not be coupled to either $\psi_1(1,1)$ or $\theta_2(1,1)$ but they get coupled to the mode $\theta_2(0,2)$ and, as a result, 5D Lorenz system is obtained. Extending this procedure to higher order vertical modes ($\psi_1(1,3)$ and $\theta_2(1,3)$), one may demonstrate that the lowest order generalized Lorenz system that can be constructed is a 9D system (see Chapter I).

I now use equations (3.1 and 3.2) to determine a rule that underlies the above selection. My analysis shows that only those vertical modes that are separated from the original Lorenz modes by 2π are coupled to the 3D system; hence , the modes with $n = 2$ are not coupled but modes with $n = 3$ are coupled. It is easy to demonstrate all the modes labeled with n being an odd integer are coupled. The situation is different for the horizontal modes as in this case all modes with m being an integer are coupled to the Lorenz modes. Hence the difference is only π. These simple rule can be used to construct a generalized Lorenz system by applying either the vertical or horizontal mode truncations. In both methods it is only required that the energy conserving modes are selected.

3.3 Routes to chaos

To determine the routes to chaos in the derived 5D system, we solved numerically the set of equations (3.3) through (3.7) by fixing parameters $b = 8/3, \sigma = 10$, and varying the control parameter over the range $0 \le r \le 30$. The calculations allowed us to establish the value of $r_{\min}$ for which the onset of chaos is observed and then determine $r_{\max}$ for which the system exhibits fully developed chaos. Routes to chaos are determined from detailed studies of the behavior of the system in the range $r_{\min} \le r \le r_{\max}$. The obtained results are presented using phase portraits, power spectra and Lyapunov spectra.

The phase space portraits for the set of variables (X , Y , Z) and (X_1 , Y_1 , Z_1) are given in figures (3.1) to (3.4) . The result presented in this figure is the time evolution of the system from given initial conditions to a periodic or a strange attractor. It is seen that the system exhibits periodic behavior for the values of 'r' ranging from 14 to 20. However, for $r = 22$, figure (3.4) display strange attractor, which shows many similarities with the original Lorenz strange attractor. The fact that the system is periodic for $r = 14 - 20$ and chaotic for $r \geq 22$ is seen in the plots of power spectra in figures 3.6 to 3.9. To determine the value of r for which the system enters chaotic regime, I plotted three Lyapunov exponents in figure 3.5. Based on these exponents, I determined $r = 21.5$ to be the critical value for the onset chaos for this 5D generalized Lorenz system. The results presented in figure 3.5 also shows that further increase of r leads to a series of spikes in Lyapunov spectra and that fully developed chaos is observed when $r = 22.5$. The spikes are typically identified as chaotic transients. Which means that is typically the route to chaos in this 5D model.

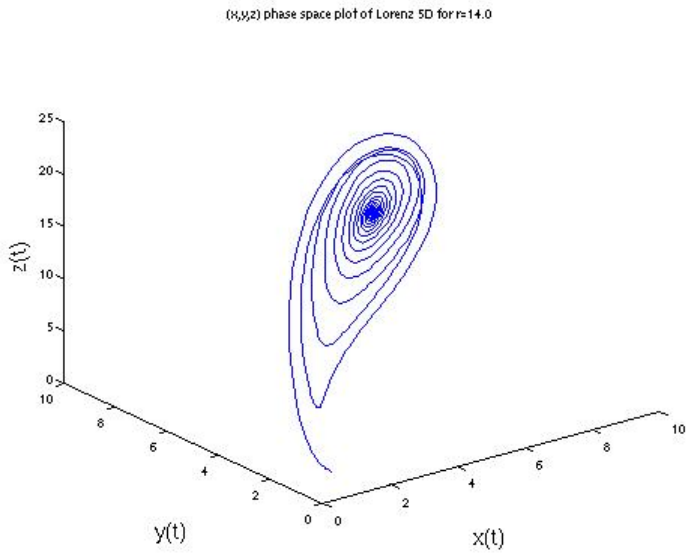

3.1 (x , y , z) phase plots at r =14.0

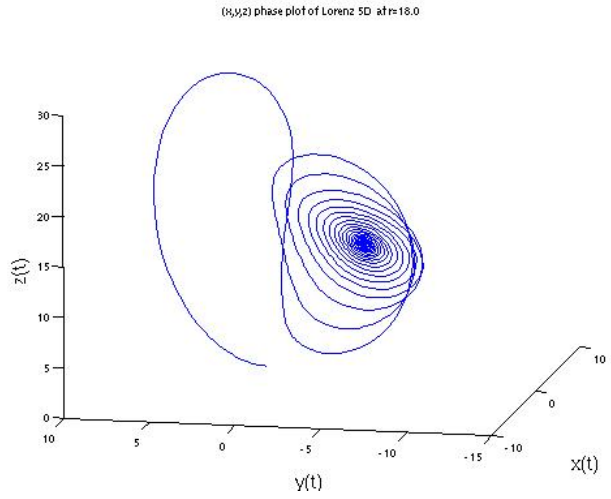

3.2 (x , y , z) phase plots at r =18.0

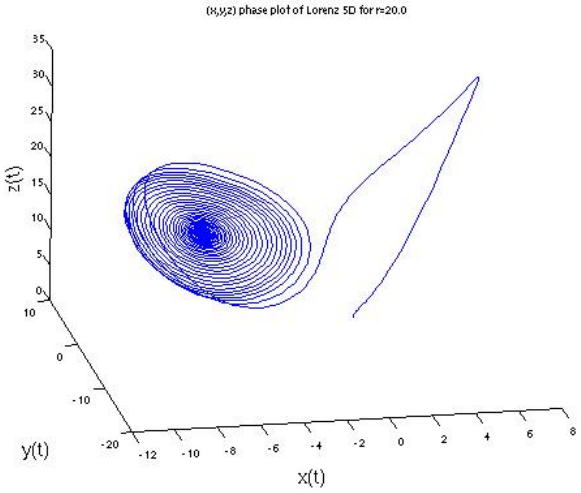

3.3 (x , y , z) phase plots at r =20.0

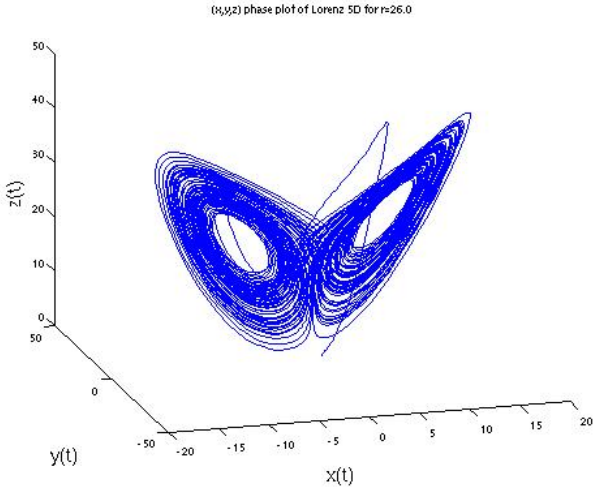

3.4 (x , y , z) phase plots at r =26.0

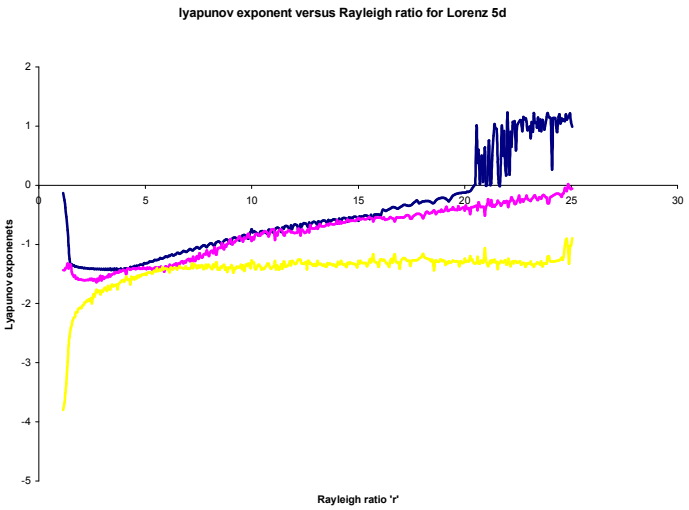

3.5 Three leading Lyapunov exponents for 5D

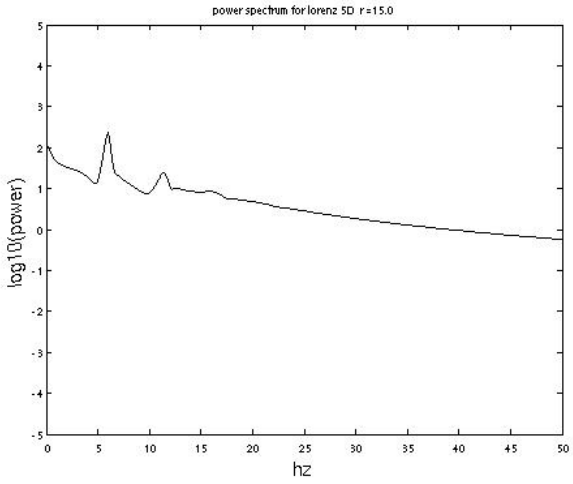

3.6 Power spectrum for Lorenz 5D at r =15.0

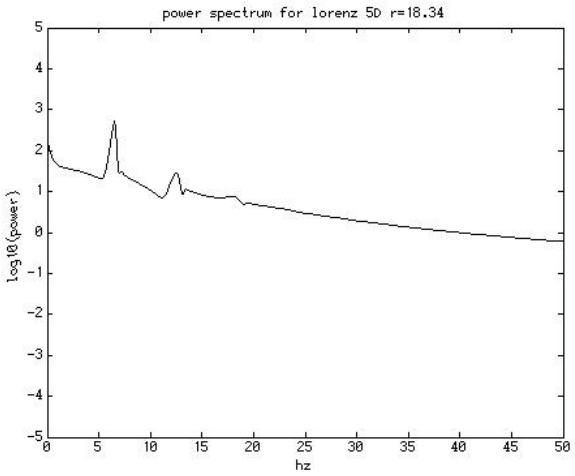

3.7 Power spectrum for Lorenz 5D at r =18.34

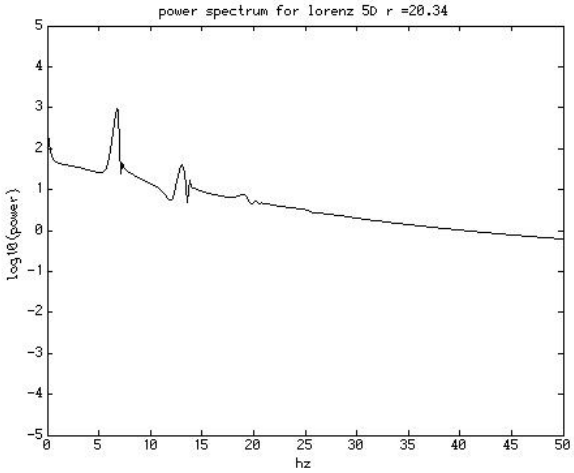

3.8 Power spectrum for Lorenz 5D at r =20.34

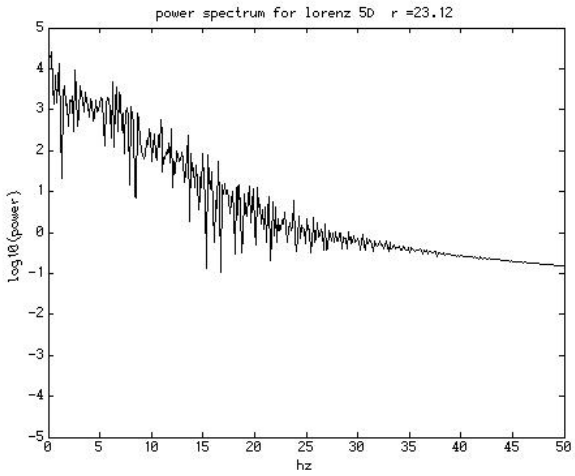

3.9 Power spectrum for Lorenz 5D at r =23.12

3.4 Comparison with other Lorenz models

I compare the above results to those previously obtained for the 3D Lorenz model and 9D Lorenz model derived in Chapter I. First of all it is seen that both the onset of chaos and the onset of fully developed chaos in the 5D system occur at the values of r that are lower than those observed in the original 3D Lorenz system and the 9D system discussed in Chapter I. To be specific, the onset of fully developed chaos in the 5D system occurs at $r = 22.5$, which must be compared to $r = 24.75$ in the 3D Lorenz model and $r = 41.54$ in the 9D model. This is a surprising result because typically the addition of higher-order modes requires higher value of r for a system to enter chaotic regime (e.g. our result in Chapter I). In the following I explain this result.

I performed studies of the role played by different Fourier modes in the onset of chaos and found out that the dominant role played by the Z modes, which represent the vertical temperature difference in the convective roll. The main result is that more

Z modes in the system the higher the value of r necessary to for the onset of chaos. Since there is only one Z mode in the 3D system and also in the 5D system, the onset of chaos for both systems takes place almost at similar values of r. However there are three Z modes in the 9D model (see chapter II) therefore the value of r required for this system to enter chaos is almost twice as high as the 5D Lorenz system. My study also shows that by adding horizontal modes to the 3D Lorenz system, the value of r required for the onset of chaos can be reduced.

To verify these conclusions I derived a 7D generalized Lorenz model by adding the following energy-conserving horizontal modes: $X_2(t) = \psi_1(3,1)$ and $Y_2(t) = \theta_2(3,1)$; Note that no Z mode was added. I investigated the onset of chaos in this model and found $r = 21.75$ to be the critical value. I also determined that at $r = 22.28$ the system enters the fully developed chaotic regime. These result supports the above conclusions. My studies show that 5D, 7D and 9D generalized Lorenz systems enter the fully developed chaos via chaotic transients. This is the same routes to chaos as observed in the original 3D Lorenz system.

CHAPTER 4

GENRALIZED LORENZ MODEL III

4.1 Horizontal-Vertical mode truncations

In this chapter a new lowest order generalized Lorenz system is derived using horizontal-vertical mode truncations. It is also found that the routes to chaos for this system changes in comparison with the models previously studied by Roy and Musielak (2006).The reasons are discussed in detail. The selection of the energy conserving modes both in horizontal-vertical directions resulted in an 8D extension of the Lorenz system. This 8D system is energy conserving in the dissipation less limit and also has bounded solutions. In order to understand the change in the routes to chaos for this system a 10D model is derived by adding two more modes to the 8D model. The numerical investigation of the 10D extension also shows the same routes to chaos as the 8D Lorenz model.

4.1.1 Introduction

Most attempts made by previous authors (J.H.Curry1978,Howard(1986), Rieterrar(1998), Humi(2004)) in order to combine the idea of coupling of lower order modes with higher order modes in the double Fourier expansions of stream function and temperature variations and in that process derive a generalized Lorenz system(1963) have failed for various reasons. I would like to point out only two important ones. (1)

Failure to select energy conserving Fourier modes (2) Failure to couple the lower order modes with higher order modes in a mathematically consistent and physically meaningful generalized Lorenz system.

In general, there are three different methods of selecting the higher-order Fourier modes (Roy 2006). In the first method, only the vertical Fourier modes are chosen. The second method is restricted to horizontal mode truncations. However, in the third method, both vertical and horizontal modes are selected. Different methods were chosen by different authors, who often made their choices without giving a clear physical justification.

In addition, in many cases Fourier modes were selected in such a way that the resulting generalized Lorenz models did not conserve energy in the dissipation less limit. The fact that the choice of the modes which do not conserve energy significantly restricts description of these systems was recognized by several authors (Thieffault(1996),Tong(2003)), who also showed how to construct energy-conserving generalized Lorenz systems.

In chapter I of this thesis, I used the first method to obtain a generalized Lorenz system. By selecting energy-conserving modes, we demonstrated that the lowest-order generalized Lorenz system was a nine-dimensional (9D) model. In paper II, I used the second method to select energy-conserving modes to construct the lowest-order generalized Lorenz model. I find that the constructed model is only five-dimensional (5D). In this chapter I derive a meaningful generalized Lorenz system by

adding three more modes with the 5 modes used to construct a 5D generalized Lorenz model. An interesting result is that the lowest order generalized Lorenz system that can be obtained using this horizontal-vertical mode variation is the 8D system. One of the reason for a 8D model is that the original Lorenz modes gets weakly coupled to two modes namely $\psi_1(2,\ 1)$ and $\Theta_2(2,\ 1)$ which are selected to derive 5D Lorenz system. Therefore, once we have constructed 5D model one can add higher order Fourier terms to derive high dimensional Lorenz system, however, one needs to be careful because the selection should be mathematically consistent and also energy conserving in the dissipation less limit. By using this criteria I obtained the 8D Lorenz system which is mathematically and physically consistent.

4.1.2 Derivation of Lorenz 8D model

Generalized Lorenz models can be derived from Saltzman's equations (see Eqs. 7 and 8 in chapter I) by taking into account different modes in the following double Fourier expansions:

$$\psi(x^*, z^*, t) = \sum_{m=-\infty}^{+\infty} \sum_{n=-\infty}^{+\infty} \psi(m, n, t^*) \exp[2\pi i h(\frac{m}{L} x^* + \frac{n}{2h} z^*)] \tag{4.1}$$

$$\theta(x^*, z^*, t) = \sum_{m=-\infty}^{+\infty} \sum_{n=-\infty}^{+\infty} \Theta(m, n, t^*) \exp[2\pi i h(\frac{m}{L} x^* + \frac{n}{2h} z^*)] \tag{4.2}$$

where x^*, y^*, z^* and t^* are dimensionless coordinates, ψ^* is the dimensionless stream function and θ^* is also a dimensionless quantity that describes temperature

variations due to convection. In addition, x and z represent the vertical and horizontal directions, respectively, L is the characteristic scale representing periodicity 2L in the horizontal direction, and h is the thickness of a convection region. Based on these expansions, we shall refer to the modes labelled by m and n as the horizontal and vertical modes, respectively.

Following Saltzman [2], we write $\psi(m, n) = \psi_1(m, n) - i\psi_2(m, n)$ and $\Theta(m, n) = \Theta_2(m, n) - i\Theta_2(m, n)$; note that the time-dependence is suppressed. Saltzman excluded all $\psi_2(m, n)$ and $\Theta_1(m, n)$ modes by fixing the vertical nodal surfaces of the convective cells, and assumed that the ψ_1 modes with m = 0 describing shear flows can be neglected. These Saltzman rules were adapted by Lorenz to construct his 3D model and by us to obtain a 9D Lorenz model in chapter I and 5D model in chapter II respectively. The same rules will be used here to derive the lowest-order generalized Lorenz system by the method of horizontal-vertical mode truncations.

4.2 Lowest order generalized model

In paper II of this series we have derived a 5D generalized Lorenz model by adding two modes namely: $\psi_1(2, 1)$ and $\Theta_2(2, 1)$ to original Lorenz modes $\psi_1(1, 1)$ that describes the circulation of a convective roll, and $\Theta_2(1, 1)$ and $\Theta_2(0, 2)$ that approximate respectively the horizontal and vertical temperature differences in the convective roll in the 3D model. I find that the above two modes (higher order) gets coupled with the lower order modes. Just like I treated original Lorenz modes as our

basis in order to add energy conserving higher order modes consistently similarly I use this 5D model that I have already derived in second chapter[16] as the basis and add higher order modes to it consistently and try to see whether they get coupled. The following higher order modes are added to achieve this objective $\psi_1(1, 2)$, $\Theta_2(1, 2)$ and $\Theta_2(0, 4)$. The last mode is added in order to satisfy the principle of conservation of energy and bounded ness of solutions. So on the basis of this truncations I was able to derive a 8D system which we find is strongly coupled with the original 3D and as well as this 5D system. I realize that Humi [10] also picked up the above modes except two of them namely: $\Theta_2(2, 1)$ and $\Theta_2(0, 4)$. I recognize that one of the modes which describes transport of the the net heat flux of the system $\Theta_2(0, 4)$ is missing from his selection of modes , the absence of this mode as shown previously by Thieffault and Horton [12] and independently by Tong et al.[14]generally affect the conservation of energy in the dissipationless limit. I would like to point out that in the method of vertical mode truncations used in chapter I the following three modes, $\psi_1(1, 2)$, $\Theta_2(1, 2)$ and $\Theta_2(0, 4)$, were added to those originally selected by Lorenz. These as I recognize are the same modes added to the 5D system. However, analysis in the first chapter showed that these modes were not coupled to the Lorenz modes and as a result we derived two independent 3D systems. In this chapter I show that these modes gets coupled to the original Lorenz modes via $\psi_1(2, 1)$ and $\Theta_2(2, 1)$ modes. Again this coupling is consistent with the rule proposed in chapter II of this thesis.

Here, I select higher-order Fourier modes by using the method of horizontal-vertical mode truncations. The original 3D Lorenz model is treated as the basis and the higher-order modes are added until the lowest-order generalized Lorenz model is obtained. I begin with the three Fourier modes $\psi_1(1,\ 2)$ and $\Theta_2(1,\ 2)$ and $\Theta_2(0,\ 4)$ which gets coupled with the original lower order Lorenz modes. The coupling resulted in the following set of ordinary differential equations:

$$\frac{dX}{d\tau} = -\sigma X + \sigma Y - (\frac{3}{4})\sqrt{2}X_1X_2 \tag{4.3}$$

$$\frac{dY}{d\tau} = -XZ + rX - Y + (\frac{3}{4})\sqrt{2}X_2Y_1 + (3/4)\sqrt{2}Y_2X_1 \tag{4.4}$$

$$\frac{dZ}{d\tau} = XY - bZ + 2X_1Y_1 \tag{4.5}$$

$$\frac{dX_1}{d\tau} = -c_1\sigma X_1 + \frac{\sigma}{c_1}2Y_1 + (\frac{3}{4})\sqrt{2}XX_2 \tag{4.6}$$

$$\frac{dY_1}{d\tau} = -2X_1Z + 2rX_1 - c_1Y_1 - (\frac{3}{4})\sqrt{2}X_2Y + (\frac{3}{4})\sqrt{2}X_1Y_2 \tag{4.7}$$

$$\frac{dX_2}{d\tau} = -c_2\sigma X_2 + \frac{\sigma}{c_2}Y_2 - \sqrt{2}(\frac{1}{4})XX_1 \tag{4.8}$$

$$\frac{dY_2}{d\tau} = -c_2Y_2 + 2rX_2 - (\frac{3}{4})\sqrt{2}XY_1 - (\frac{3}{4})\sqrt{2}X_1Y - 2X_2Z_1 \tag{4.9}$$

$$\frac{dZ_1}{d\tau} = 2X_2Y_2 - 4bZ_1 \tag{4.10}$$

Where X(t) = ψ_1 (1, 1), Y (t) = $\Theta_2(1,\ 1)$, Z(t) = $\Theta_2(0,\ 2)$, $X_1(t)$ = $\psi_1(2,\ 1)$,

$Y_1(t) = \Theta_2(2, 1)$, $X_2(t) = \psi_1(1, 2)$, $Y_2(t) = \Theta_2(1, 2)$ and $Z_1(t) = \Theta_2(0, 4)$. In addition, $\tau = 2(1+a^2)t$ is dimensionless time, a = h/L is the aspect ratio, b = 4/(1 + a2), r = $\frac{R}{R_c}$ with $R_c = \pi^4(1 + a^2)^3/a^2$, and c1 = $(1 + 4a^2)/(1 + a^2)$, c2 = $(4 + a^2)/(1 + a^2)$.

When we observe this constructed 8D model we find that all the selected modes are fairly strongly coupled to each other. As we will show in the next section the extra terms that results in (3),(6) and (8) cancels out among each other resulting in a bounded and energy conserving solutions. As expected, the model reduces to the 5D Lorenz model when $X_2 = Y_2 = Z_1 = 0$. A natural question is whether this derived model is needed a generalized lowest order Lorenz model. To answer this question all I did let $Z_1(t) = 0$, Therefore either $X_2(t) = 0$ or $Y_2(t) = 0$ in (10). In either case one can easily show that this results into a 6D Lorenz system. However, there still remains an ambiguity regarding the fact that which modes among $X_2(t)$ and $Y_2(t)$ should be retained in the Fourier expansion which is precisely the reason that lacks in Humi's derivation of his 6D model (2004). We try to resolve this ambiguity here by invoking energy conservation principle presented by Thiffeault and Horton (1996) and by selecting following energy conserving modes $X_2(t), Y_2(t)$ and Z_1(t). Therefore we conclude that the derived 8D system is indeed the lowest order generalized Lorenz system by using Horizontal-vertical mode truncations. Now, we may use the method presented in Paper I (see Sec. II.C) to show that the derived 8D model conserves energy

in the dissipation less limit and has bounded solutions. As a result, we call the modes $X_2(t) = \psi_1(1, 2)$ and $Y_2(t) = \Theta_2(1, 2)$ and $Z_1(t) = \Theta_2(0, 4)$ as the energy-conserving modes.

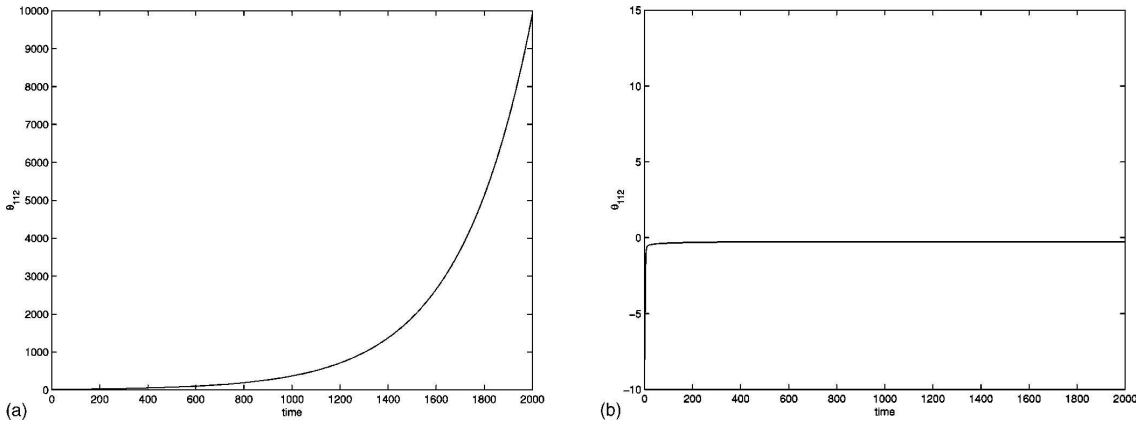

4.1 Time series plot for model I and model II

4.3 Energy conservation of 8D model

The equations for kinetic and potential energy can be written using the following expressions:

$$K^* = \frac{1}{2}\sum_{m=-\infty}^{+\infty}\sum_{n=-\infty}^{+\infty}\delta^2(m,n)\psi^2(m,n) \tag{4.11}$$

$$U^* = -(\frac{1}{2})\frac{\sigma}{R}\sum_{m=-\infty}^{+\infty}\sum_{n=-\infty}^{+\infty}\Theta^2(m,n) \tag{4.12}$$

where $\delta^2(m,n) = m^2a^2 + n^2$

The quantity is already normalized. we apply this above mentioned formula to our 8D system to obtain

$$K^* = \frac{1}{2}[\delta^2(1,1)\psi^2(1,1) + \delta^2(2,1)\psi^2(2,1) + \delta^2(1,2)\psi^2(1,2)] \tag{4.13}$$

$$U^* = -\frac{1}{2}\frac{\sigma}{R}[\Theta^2(1,1) + \Theta^2(2,1) + \Theta^2(1,2) + \Theta^2(0,2) + \Theta^2(0,4)] \tag{4.14}$$

where $\delta^2(1,1)$, $\delta^2(2,1)$ and $\delta^2(1,2)$ are constants.

To show that the total energy, $E^* = K^* + U^*$, is indeed conserved in the dissipation less limit I write the following expression for total energy

$$\begin{aligned}\frac{dE^*}{d\tau} &= -\sigma[\delta^2(1,1)(X-Y) + \delta^2(2,1)(c_1X_1 - \frac{2}{c_1}Y_1) + \delta^2(1,2)(c_2X_2 - \frac{2}{c_2}Y_2)] \\ &-\delta^2(1,1)(\frac{3}{4})\sqrt{2}XX_1 + \delta^2(2,1)(\frac{3}{4})\sqrt{2}X_1X_2 - \delta^2(1,2)(\frac{1}{4})\sqrt{2}XX_1 \\ &-\frac{\sigma}{R}[\dot{Y} + \dot{Y}_1 + \dot{Y}_2 + \dot{Z} + \dot{Z}_1]\end{aligned} \tag{4.15}$$

In the dissipation less limit $\sigma \to 0$ the above Equation (4.15) gives

$$\lim_{\sigma \to 0}\frac{dE^*}{d\tau} = 0 \tag{4.16}$$

Which gives $E^* = K^* + U^*$ = const. Hence, our 8D system conserves energy in the dissipation less limit.

4.4 Routes to chaos

To determine route to chaos in the derived 8D system, we solved numerically the set of equations (3) through (10) by fixing the parameters b = 8/3 and _ = 10, and varying the control parameter r over the range $0 \le r \le 40$. The calculations allowed us to

establish the value of r min for which the onset of chaos is observed and then determine r max for which the system exhibits fully developed chaos. Route to chaos is determined from detailed studies of the behavior of the system in the range $r\,\min \le r \le r\,\max$. The obtained results are presented using phase portraits, power spectra and Lyapunov spectra.

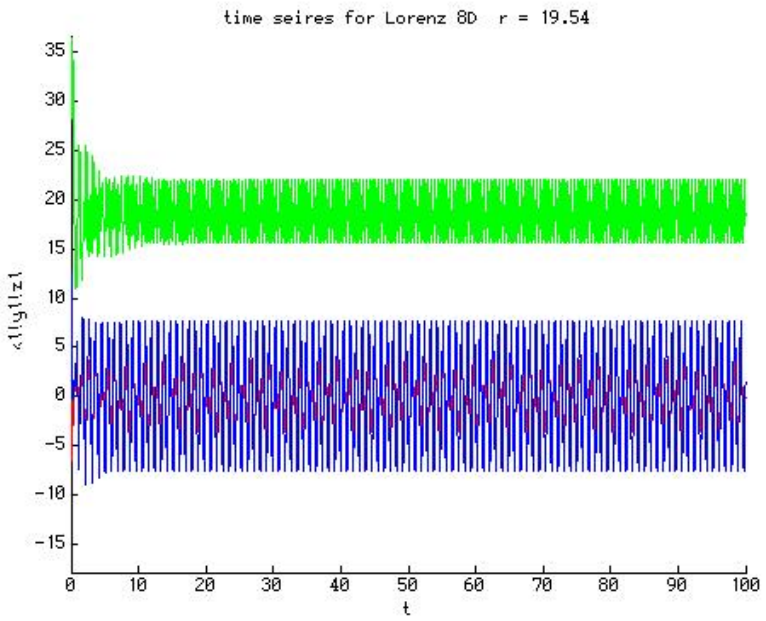

4.2 Time series plot for x1, y1, z for 8D at r =19.54

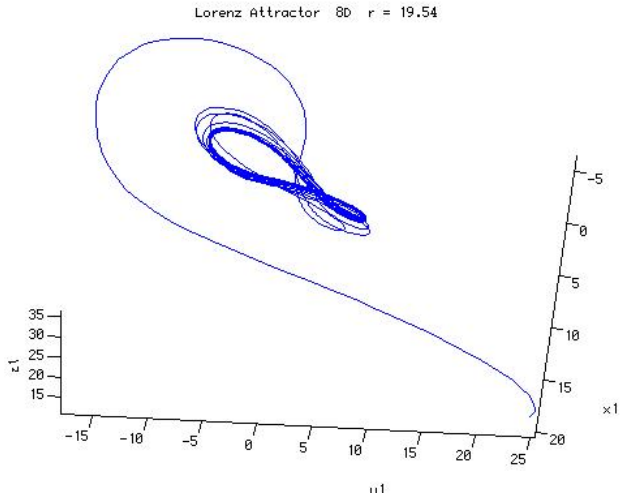

4.3 Phase space portrait for x1, y1, z at r =19.54

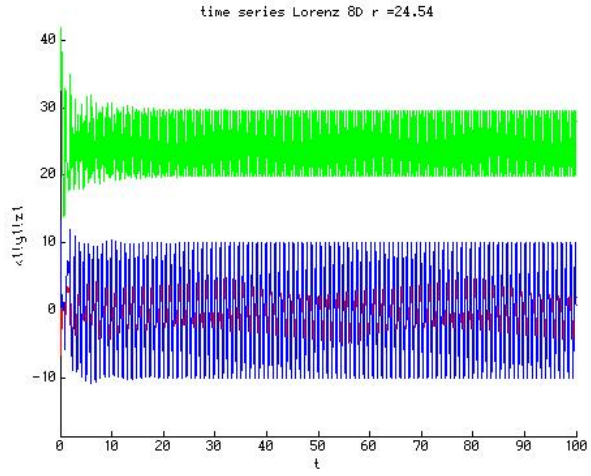

4.4 Time series plot for x1, y1, z for 8D at r =24.54

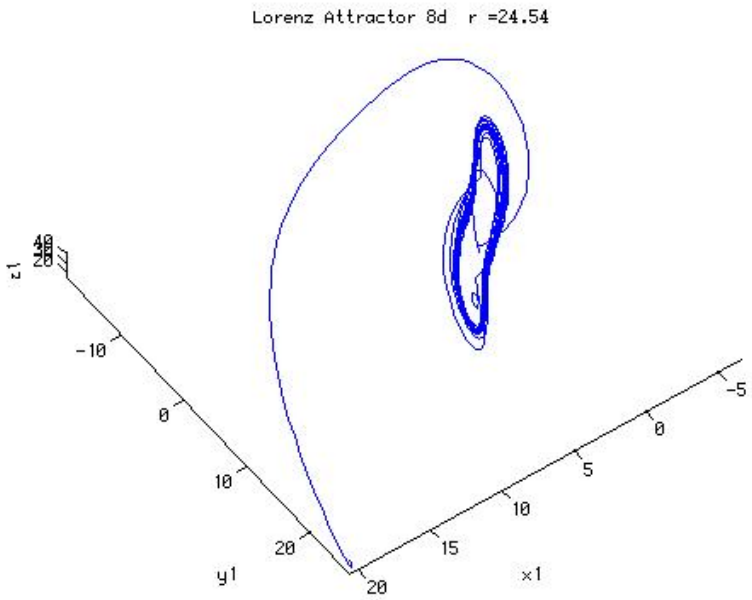

4.5 Phase space portrait for x1, y1, z at r =24.54

The phase portraits and time series for the sets of variables (X, Y, Z) and (X1, Y1, Z) are given in Figures (4.1) through (4.4). The result presented in these figures show time evolution of the system from given initial conditions to a periodic or strange attractor. It is seen that the system exhibits periodic behavior for the values of r ranging from 15 to 36. However, for r = 36, the figure (4.7) displays a strange attractor, which shows differences and as well as similarities to the original Lorenz attractor. The quasi periodic behavior of this system is quite nicely captured in the power spectral plot for value of r = 15 − 35 and chaotic for r = 36.54 is seen in plots of the power spectra given in Figs 4.10 through 4.12. In order to exactly determine the value of r for which the system enters the chaotic regime, we plotted three leading Lyapunov exponents in Fig.

4.9. Based on these exponents, we were able to establish that at r = 32.5 − 34.5 all three leading Lyapunov exponents becomes zero and therefore supports our argument about the quasi periodic behavior of this dynamical system.

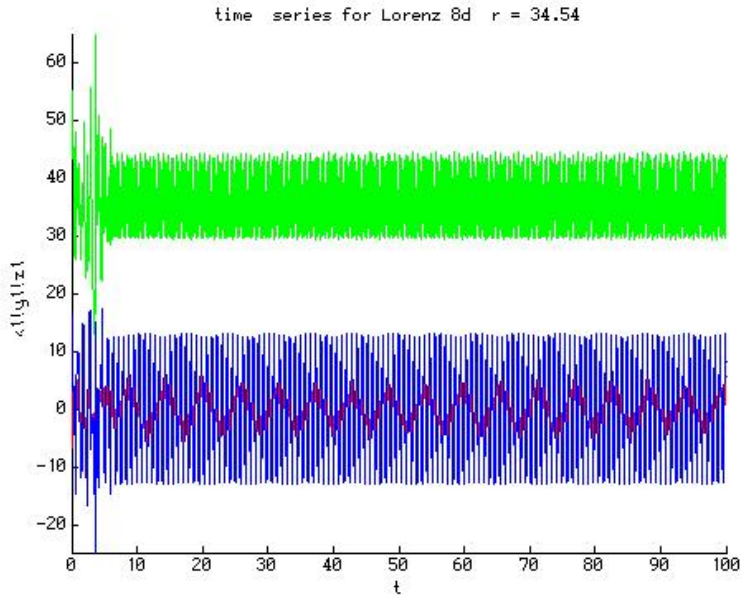

4.6 Time series plot for x1, y1, z for 8D at r =34.54

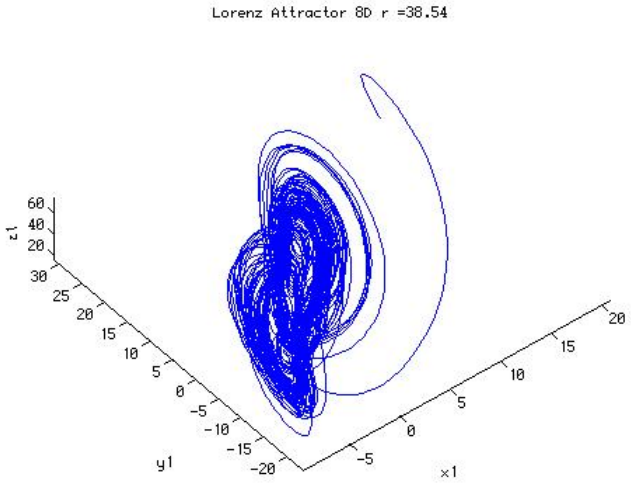

4.7 Phase space portrait for x1, y1, z at r =38.54

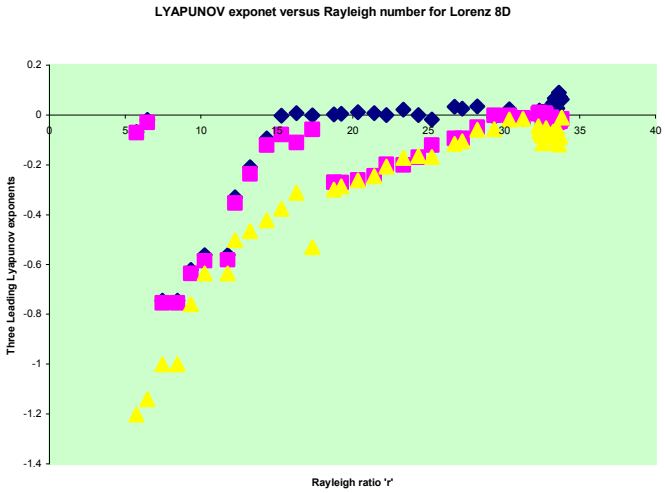

4.8 The leading three Lyapunov exponents

I investigated the behavior of both Lyapunov exponents and power spectral plot in the range of values between r = 32.5 − 34.5 just to understand how and what value the quasi periodic behavior decays to chaotic behavior. we were able to show based on our numerical results that the system enters chaotic regime at r = 35.5.The results presented in Fig. 7 also show that further increase of r leads to almost linear increase of leading Lyapunov exponent and the other two Lyapunov exponents becomes negative .In this process the fully developed chaos is observed when r = 36.5. These results allow us to conclude that the routes to chaos for this 8D system is the following $T_0 \to T_1 \to T_2 \to T_3 \to chaos$.

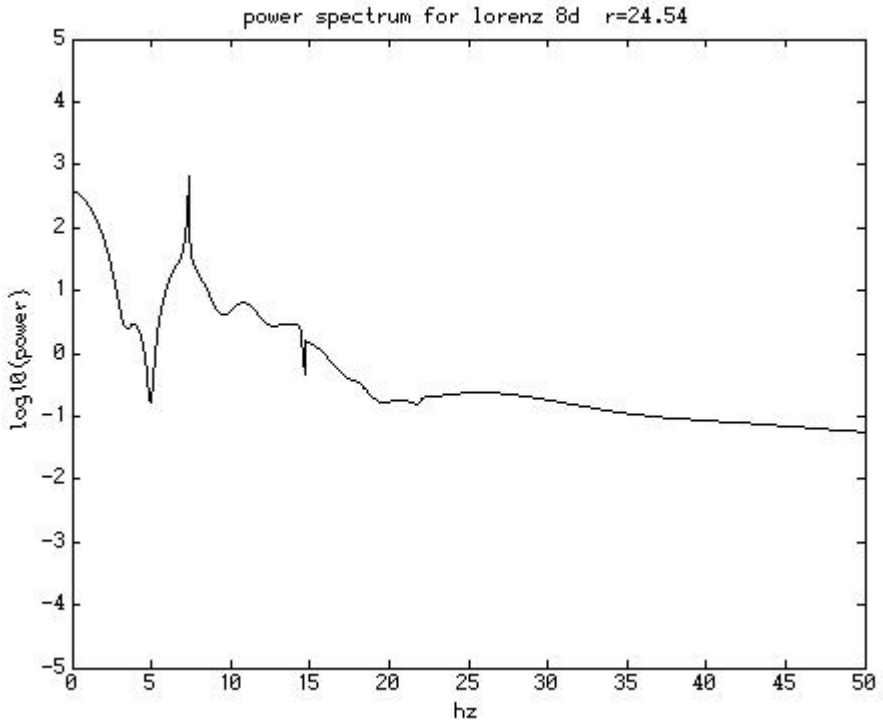

4.9 Power spectral plot for 8D at r =24.54

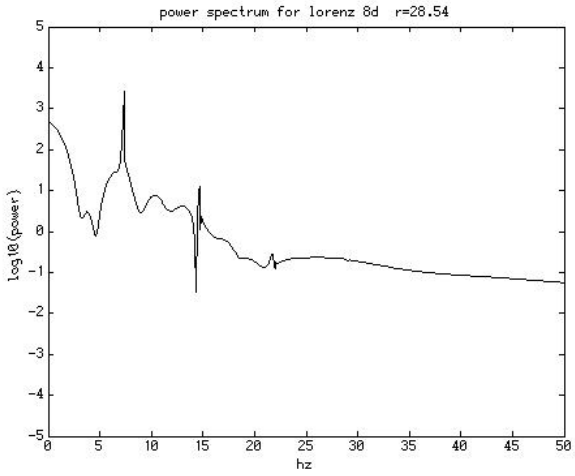

4.10 Power spectral plot for 8D at r =28.54

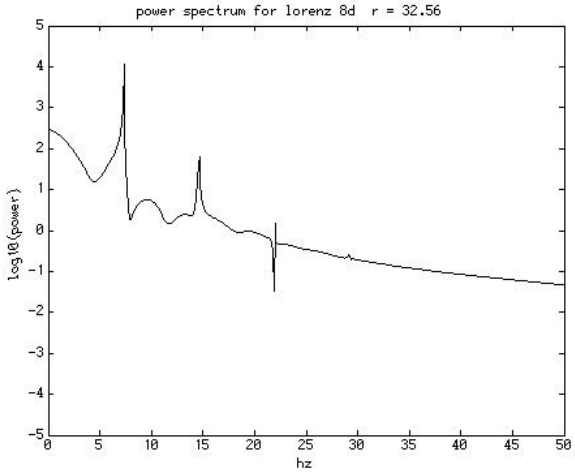

4.11 Power spectral plot for 8D at r =32.56

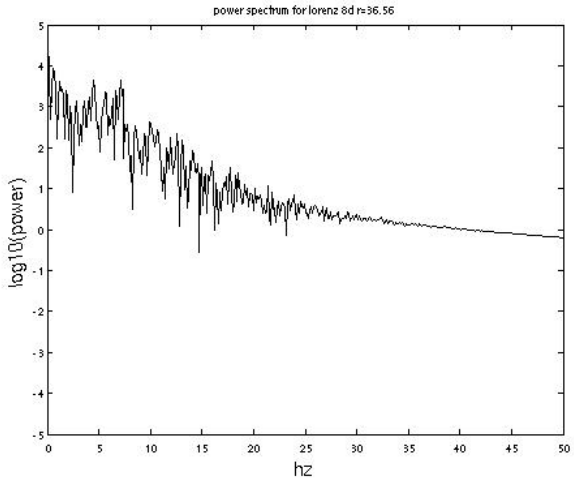

4.12 Power spectral plot for 8D at r =36.56

In order to understand this behavior clearly I derived a 10D Lorenz model by adding both horizontal and vertical modes to this 8D system. I observe that in order to derive this 10D model one can either add two following modes $X_3(t) = \psi_1(2,2)$ and $Y_3(t) = \Theta_2(2,2)$ or $X_3(t) = \psi_1(3,1)$ and $Y_3(t) = \Theta_2(3,1)$ to the modes already selected based on energy conservation to derive 8D system. However, the selection of first two modes gives extraneous terms which do not cancel out in the dissipation less limit therefore one must add the next two modes in order to derive a 10D system. We investigated our 10D system numerically and found that the routes to chaos for this system is also through quasi periodicity. Moreover we find that the critical value of r = 35.5 for the onset of chaos in this 10D system which is in agreement with our observation in chapter II of this thesis. Therefore, based on these results I conclude that

one of the main reasons the routes to chaos changes in the 8D system compared with our previous models is because of the strong coupling between all the selected modes and the same is also true for the 10D system.

4.5 Comparisons with other Lorenz models

We now compare the above results to those previously obtained for the 9D generalized Lorenz systems and the 5D generalized Lorenz system discussed in chapter I and chapter II. First of all, it is seen that both the onset of chaos and the onset of fully developed chaos in the 5D system occur at the values of r that are lower than those observed for the original 3D Lorenz system and the 9D system discussed in Paper I. To be specific, the onset of fully developed chaos in the 5D system occurs at r = 22.5, which must be compared to r = 24.75 in the 3D Lorenz model and r = 41.54 in the 9D model. In this 8D system the onset of chaos occurs at r = 36.5 which is consistent with our observation in chapter II. We performed studies of the role played by different Fourier modes in the onset of chaos and found out that the dominant role is played by the Z modes, which represent the vertical temperature difference in a convective roll. The main result is that the more Z modes in the system, the higher the value of r required for the onset of chaos. Since there is only one Z mode in the 3D Lorenz system and also one Z mode in the 5D system, the onset of chaos in both systems takes place at similar values of r. However, there are three Z modes in the 9D system (see chapter I), so the value of r required for this system to enter chaos is almost twice as high as that

observed in the 5D system. Similarly the r value required for the onset of chaos in the 8D system is also high compared to previously studied 5D model(see chapter II) and low in comparison with the 9D model(see chapter I). My studies also showed that by adding both horizontal and vertical modes to the 5D Lorenz system, I was able to derive a system which is fairly strongly coupled as a result it's collective behavior is entirely different from the 5D system. To be precise we observe that $X(t), X_1(t), X_2(t)$ gets coupled with each other in the respective differential equations which is not the case with 9D or 5D system. Moreover this modes gets also fairly well coupled with the Y (t), Y1(t) and Y2(t) modes and as well as with Z(t) providing just the right additional stability to the system. This I perceive as one of the main reason for the routes to chaos for this system to become quasi periodic. To verify this hypothesis, we derived a 10D generalized Lorenz model by adding the following energy-conserving horizontal modes: $X_3(t) = \psi_1(3,1)$ and $Y_3(t) = \Theta_2(3,1)$; note that no Z mode was added. We investigated the onset of chaos in this model and found r = 35.5 to be the critical value. We also determined that at r = 36.28 the system enter the fully developed chaotic regime through quasi periodicity. These results support the above hypothesis.

My studies showed that the 8D and 10D generalized Lorenz systems enter the fully developed chaotic regime via quasi periodicity this is different from the route to chaos as that observed in the original 3D Lorenz system.

CHAPTER 5

SUMMARY OF THESIS

I used the method of the vertical mode truncation in chapter I to construct generalized Lorenz models that approximate a 2D Rayleigh-B´enard convection. The original 3D Lorenz model is a subset of these models, which means that the generalized systems were derived by adding higher order Fourier modes to the original three modes selected by Lorenz (1963). An interesting result of my study is that the lowest-order generalized Lorenz model, which conserves energy in the dissipation less limit and has bounded solutions, is a 9D system and that its route to chaos is via chaotic transients, first observed in the 3D Lorenz system. In addition, it is shown that more thermal energy is required for our 9D system to transition to chaos than for the 3D Lorenz system. The critical value of r for which our system exhibits fully developed chaos is r = 41.54, however, it is only r = 24.75 for the 3D system. This implies that the larger number of Fourier modes are taken into account, the higher the values of r are required for the system to enter the fully developed chaotic regime. The method of the vertical mode truncation did not allow us to construct any physically consistent system with dimensions ranging from four to eight. There are, however, some examples of such models constructed by others (Kennamer (1995), Humi (2004), Howard (1986)). One example is a 6D system developed by Kennamer (1995). There are similarities between

this energy-conserving model and our 9D system, namely, both models have strange attractors that have properties very similar to the Lorenz strange attractor and chaotic transients are their routes to chaos. However, the problem is that the 6D model was derived by skipping the vertical modes with m = 1 and n = 2 and selecting a temperature mode with m = 0 and n = 4 in an inconsistent way (Tong (2003)). Other 6D and 9D models (Humi (2004), Reiterer (1998)), which predicted period-doubling as their routes to chaos, happened to be non-conserving energy systems. Similarly, it has been shown that a 14D model constructed by Curry (1978), with its route to chaos via decaying tori, does not conserve energy in the dissipation less limit.

Based on our results and their comparison to those previously obtained, it is now clear that the period-doubling route to chaos discovered by Humi (2004) and Reiterer (1998) in their generalized Lorenz models was caused by their selection of the modes that do not conserve energy. The same is true for the 14D system constructed by Curry (1978) as this system also voliates the principle of the conservation of energy. On the other hand, my results clearly show that when genearlized Lorenz models are constructed in such a way that the energy-conserving Fourier modes are taken into account, then the route to chaos in these models is the same (chaotic transients) as that observed in the original 3D Lorenz model.

The method of horizontal mode truncations was used in chapter II to construct generalized Lorenz systems by selecting energy-conserving modes. The main result is that a 5D system is the lowest-order generalized Lorenz model, which can be constructed by this method. In chapter I it is showed that a 9D system is the lowest-

order generalized Lorenz model that can be constructed by the method of vertical mode truncations (see chapter I). This implies that horizontal modes couple more easily to the original 3D Lorenz system than the vertical modes. The general rule is that all (even and odd) horizontal modes are coupled but among all vertical modes only the odd modes get coupled.

My numerical studies of the 5D system showed that the onset of chaos in this system occurs at value of r = 21.5, which is lower than that required for the onset of chaos in the 3D Lorenz system. The onset of fully developed chaos takes place at r = 22.5, which is lower than r = 24.75 for the 3D Lorenz model and r = 41.54 for the 9D model. I demonstrated that the value of r for which the onset of chaos occurs is primarily determined by a number of z modes in a system. These modes represent the vertical temperature variations resulting from the convection and more of them in a system require higher values of r for the onset of chaos. My results also showed that the 5D system transitions to chaos via chaotic transients, which is the same route to chaos as that observed in the 3D Lorenz system and in the 9D system. This clearly shows that the route to chaos in the lowest-order generalized Lorenz systems remains the same as in the original Lorenz system. The lowest order generalized Lorenz system is constructed in chapter III based on the horizontal-vertical mode truncations. The main result is that the lowest order generalized Lorenz system is a 8D system in this method of truncations and that all the selected modes in the Fourier double expansion are fairly well coupled with each other resulting in the collective dynamics of the system as the

parameter r is varied. The onset of chaos occurs at higher r values which is the result of selection of higher z modes. My previous work showed that based on the method of horizontal and vertical mode truncations one can derive a 5D and 9D model respectively and that the routes to chaos remain the same as in the original Lorenz 3D model. The main conclusion is that 3D, 5D, 7D and 9D models show the same routes to chaos. On the other hand 8D and10D models show different routes to chaos in comparison with the above models. Therefore it is clear that the horizontal-vertical mode truncations lead to a different route to chaos. The physical reason for this change in the route to chaos is discussed in section D of chapter 4. I further argue that by using the method of horizontal-vertical mode truncations one can derive higher dimensional Lorenz systems and perhaps would be able to understand the rule by which the higher order modes get coupled with the lower order modes. This requires further research.

5.1 Future work and recommendations

The results of this thesis can be extended to high dimensional systems. One can use energy conserving horizontal-vertical mode truncations to derive higher dimensional generalized Lorenz model to study the onset of chaos. One can further investigate the route to chaos for the derived models and try to find out if there exist any correlation between the dimension and the route to chaos. One can also explore the possibility of discovering a new route to chaos in the derived high dimensional models. Future work requires a study to the applicability of the method for other systems.

APPENDIX A

ENERGY CONSERVATION THEOREM

In general the Fourier expansion of the nonlinear equations can be infinite dimensional and therefore one can have infinite number of conserved quantities in the limit $\nu \to 0, \kappa \to 0$. Here I shall concern myself with the total energy, E, given by

$$E = \frac{1}{2}\left\langle (\psi)^2 \right\rangle - \left\langle yT \right\rangle = K + U \ , \qquad \text{(A.1)}$$

where K is the kinetic energy, U is the potential energy, and the angle brackets denote the integral over the fluid domain. In the dissipationless limit, the time derivative of E is

$$\frac{dE}{dt} = -\left\langle \psi \frac{\partial}{\partial t} \nabla^2 \psi \right\rangle - \left\langle y \frac{\partial T}{\partial t} \right\rangle = 0 \qquad \text{(A.2)}$$

showing that the total energy is conserved (I have set surface terms to zero in Equation. 4). The total internal (thermal) energy of the fluid, $\left\langle T \right\rangle$, is also conserved.

Let me now look at truncations of system (1) and their properties. In the first part we derive the equations of motion for modes of the truncations. I also examine the behavior of the invariants after they are truncated and show that they can be made to remain invariant by adding certain modes to the system. Such truncations will be called energy-conserving. Finally, I examine the important properties of these truncations, namely that the truncated system has no singular solutions and that the thermal flux is properly modeled.

To turn the system of partial differential equations (1) into ordinary differential equations, we use the following normal mode expansions for the ψ and T fields:

$$\psi(x,y,t) = \sum_{(m,n)\in A_\psi} \psi_{m,n} e^{i(m\alpha x + ny)}, \tag{A.3}$$

$$T(x,y,t) = \sum_{(m,n)\in A_\psi} T_{m,n} e^{i(m\alpha x + ny)}, \tag{A.4}$$

where $\alpha = (1/L)$ is the inverse aspect ratio. The summations are over some sets A_T and A_ψ modes (i.e., (m, n) pairs, where both m and n can be negative or zero). If both of these sets are infinite and contain all possible (m,n) pairs, then the equalities hold. Otherwise, the expansion is a truncation. Expansion (A.3 and A.4) are more general than used by previous authors (Humi (2004), Curry (1978)): first, it allows for a variable phase in the rolls (by allowing the m, n to be complex) and second, the expansion admits a non-vanishing shear flow part (the $\psi_{0,n}$ modes). The reality of the fields and the stress-free boundary conditions (2) lead to

$$\psi_{m,n} = \psi^*_{-m,-n} = -\psi_{m,-n} \tag{A.5}$$

$$T_{m,n} = T^*_{-m,-n} = -T_{m,-n} \tag{A.6}$$

so that if, say, $\psi_{1,1}$ is in A_ψ , then so are $\psi_{1,-1}, \psi_{-1,1}$ and $\psi_{-1,-1}$ similarly for A_T . Note that A_ψ and A_T need not contain the same modes. For convenience I define $\rho_{m,n} = \alpha^2 m^2 + n^2$ to be the eigenvalues of the operator $-\nabla^2$. If I insert Equation (A.5) into the Boussinesq equation (1), we obtain the following set of coupled nonlinear ODE's:

$$\frac{d\psi_{m,n}}{dt} = -\nu\rho_{m,n}\psi_{m,n} - i\frac{\alpha m}{\rho_{m,n}}T_{m,n} + \sum_{\substack{m'+m''=m \\ n'+n''=n}} \alpha(m'n'' - m''n')\frac{\rho_{m'',n''}}{\rho_{m,n}}\psi_{m',n'}\psi_{m'',n''} \qquad \text{(A.7)}$$

$$\frac{dT_{m,n}}{dt} = -\kappa\rho_{m,n}T_{m,n} + i\alpha m\psi_{m,n} + \sum_{\substack{m'+m''=m \\ n'+n''=n}} \alpha(m'n'' - m''n')\psi_{m',n'}T_{m'',n''} \qquad \text{(A.8)}$$

The kinetic and potential energies given by Equation. (A.3) have the expansions

$$K = \frac{1}{2}\sum_{m,n}\rho_{m,n}\psi^2{}_{m,n} \qquad \text{(A.9)}$$

$$U = i\sum_{p\neq 0}\frac{(-1)^p}{p}T_{0p} \qquad \text{(A.10)}$$

One can ask whether the total energy E is still conserved in the dissipation less limit for a truncated system. Taking the time derivative of Equations. (A.9 and A.10) and using Equations. (A.7 and A.8) with $\nu = \kappa = 0$,

I obtain after some manipulation:

$$\frac{dE}{dt} = \frac{d(K+U)}{dt} = i\alpha\sum_{m,n} m\psi_{m,n}T^*{}_{m,n} + i\alpha\sum_{\substack{m,n \\ p\neq 0}}(-1)^p m\psi_{m,n}T^*{}_{m,n-p} \qquad \text{(A.11)}$$

Let N ≡ {max (n) | (m, n)$\in A_\psi \cup A_T$} i.e., the maximum vertical mode number included in the truncation. If one assume the sum over p runs from −N′ to N′, one can write Equation. (A.11) as

$$\frac{dE}{dt} = i\alpha\sum_{m}\sum_{n=-N}^{N}\sum_{p=-N'}^{N'}(-1)^p m\psi_{m,n}T^*{}_{m,n-p} \qquad \text{(A.12)}$$

Now replace p by s = n − p:

$$\frac{dE}{dt} = i\alpha\sum_{m}\sum_{n=-N}^{N}\sum_{s=-N'+n}^{N'+n}(-1)^{n-s} m\psi_{m,n}T^*{}_{m,s} \qquad \text{(A.13)}$$

where the maximum lower bound for s is −N′ + N when n = N, while the minimum upper bound is N′ − N when n = −N. If N′ = 2N, s $\in [-N, N]$ always (since for |s| > N the mode is not included in the truncation and so it must vanish), and one can use the symmetries given by Equation. (A.5 and A.6) to show that $\frac{dE}{dt}$ vanishes. Hence, p has to run from −2N to 2N, which implies adding the modes $T_{0,-2N}$ . . . $T_{0,2N}$ to A_T . For the internal energy, $\langle T \rangle$, the expansion is

$$\langle T \rangle = \frac{2i}{\pi} \sum_{podd} \frac{T_{0p}}{p} \tag{A.14}$$

and its time derivative in the dissipation less limit is

$$\frac{d\langle T \rangle}{dt} = \frac{2\alpha i}{\pi} \sum_{m,n} \sum_{podd} m\psi_{m,n} T^*_{m,n-p} \tag{A.15}$$

Comparing equation. (A.15) with equation. (A.11), I see that the equation. (15) vanishes under the same condition as the total energy E.

To show that the truncated systems obtained have bounded solutions for all times t > 0, we consider the quantity Q:

$$Q = K + 2 \sum_{m,n>0} \left| T_{m,n} \right|^2 + \sum_{n>0} (T^i{}_{0,n} - \frac{2}{n})^2 \tag{A.16}$$

where K is the kinetic energy defined previously. The quantity Q is non-negative and it includes all the modes in the truncation such that if any of them diverges, then Q

diverges. Thus, if Q is bounded from above then the truncated system has no unbounded solutions.

Taking the time derivative of Q, with the viscosity and thermal conductivity nonzero, we can write:

$$\frac{dQ}{dt} \leq -\min\{2\nu, \kappa\}Q + 4\kappa N_0 \tag{A.17}$$

with N_0 being the number of $T_{0|n|}$ modes included in the truncation. For Q > $\frac{4\kappa N_0}{\min\{2\nu, \kappa\}}$, I have $\frac{dQ}{dt}$ < 0, and so Q is bounded. One can define the horizontally averaged vertical thermal flux as $q(y) = q_{cv}(y) + q_{cd}(y)$, where $q_{cv}(y) = \overline{v_y T}$ is the convective thermal flux and $q_{cd}(y) = \kappa(1 - \overline{\partial_y T})$ is the conductive thermal flux (the bar denotes an average over x). For energy-conserving truncations one can write the expansion for q as :

$$q(y) = \langle q \rangle - 2\sum_{m>0} \frac{\cos my}{m} \frac{dT^i{}_{0,n}}{dt} \tag{A.18}$$

In a steady-state situation this reduces to the expected result q = $\langle q \rangle$, independent of y, showing that the energy cannot "pile up" in steady convection. For a general truncation, one cannot write q in the form given by Equation. (18) and the thermal flux has an unphysical y dependence in a steady-state. General truncations can also have unbounded solutions as is the case in (Howard (1986)) for large enough Rayleigh number.

APPENDIX B

FORTRAN CODE FOR LYAPUNOV EXPONENTS

Program Lyapunov exponents estimation

```
c
c pini-initial prandl number,tau-incremental integration step
c b-aspect ratio,Nmax=integration points
c r-Rayleigh ratio,T-TIME
c maxstepsr=rsteps,NLE=OF SYSTEM OF DIFFERENTIAL EQUATIONS
c NE=OF SYSTEM AND LINEARIZED EQUATIONS
c Toll-exponent tolerance
c
INTEGER I,NMAX,NE,NLE,K,MAXRSTP,IR,CT,kk,ij
PARAMETER(NMAX=1000,NLE=8,MAXRSTP=100)
REAL b,r,tau,y(72),dydx(72),sigma,ex1,ex2,ex3,ex(nle),exold(nle)
real znorm(nle),gsc(nle),cum(nle),delr,rinti,pini,t,toll(nle)
real epsl(nle),eps
common sigma,b,ne
open(unit=11,file='lyap3.dat',status='unknown')
data tau,eps,delr,rinti,pini/.005,.001,.05,32.74,10.0/
b=8.0/3.0
ne=30
r=rinti
sigma=pini
do 14 i=1,nle
```

```
epsl(i)=eps
14    continue
      do 500 ir=1,maxrstp
       r=r+delr
       y(1)=10.
       y(2)=5.
       y(3)=15.
       y(4)=20.
       y(5)=25.
       y(6)=30.
       y(7)=35.
       y(8)=40.

      do 5 i=1,nle
       ex(i)=0.0
       exold(i)=1.0
       y((nle+1)*i)=1.0
       cum(i)=0.0
5     continue

      t=0.0
      ct=0
```

```
      do 250 i=1,nmax
      t=float(i)*tau
      do 6 ij=1,nle
      exold(nle)=ex(nle)
6     continue
call rk(y,dydx,tau,r)
call ornorm(nle,y,cum,gsc,znorm,ex,t)
do 128 k=1,nle
if (k.eq.1) then
ex1=ex(k)
elseif(k.eq.2)then
ex2=ex(k)
elseif(k.eq.3)then
ex3=ex(k)
elseif(k.eq.4)then
ex4=ex(k)
elseif(k.eq.5)then
ex5=ex(k)
c    explot=ex3
       endif
 128   continue
```

```
c    write(*,*)r,t,ex1,ex2,ex3
c    if((ex2.lt.eps).and.(ex2.gt.-eps))then
c    write(9,98)ct,r,ex1,ex2,ex3
c
c   goto 500
c   explot=0.0
c  endif
if(i.eq.nmax)then
ct=1
write(11,*)r,ex1,ex2,ex3,ex4,ex5
goto 500
endif
do 125 k=1,nle
toll(k)=abs(ex(k)-exold(k))
125    continue

      do 127 kk=1,nle
      if(toll(kk).ge.epsl(kk))then
      goto 250
      endif
127    continue
```

```
      write(11,*)r,ex1,ex2,ex3,ex4,ex5
      goto 500
250   continue
500   continue
      stop
      end
c


c     integration subroutine
c
      subroutine rk(y,dydx,tau,r)
      real y(72),dydx(72),tau,y1(72),dydx2(72),dydx3(72),dydx4(72),r
      integer i
      common sigma,b,ne
      call dervs(y,dydx,r,tau)
        do 10 i=1,72
         y1(i)=y(i)+.5*dydx(i)
10     continue
call dervs(y1,dydx2,r,tau)
do 20 i=1,72
y1(i)=y(i)+.5*dydx2(i)
20      continue
```

```
      call dervs(y1,dydx3,r,tau)
       do 30 i=1,72
       y1(i)=y(i)+dydx3(i)
30     continue
      call dervs(y1,dydx4,r,tau)
       do 50 i=1,72
       y(i)=y(i)+(1./6.)*(dydx(i)+2.*dydx2(i)+2.*dydx3(i)+dydx4(i))
50     continue
      return
      end

c
c  linearized system of equations to be solved

      subroutine dervs(y,dydx,r,tau)
      real y(72),dydx(72),r,tau
      common sigma,b,ne
      dydx(1)=tau*(-sigma*y(1)+sigma*y(2)-(3/4)*1.41*y(4)*y(6))
      dydx(2)=tau*(-y(1)*y(3)+r*y(1)-y(2)+(3/4)*1.41*y(4)*y(7)
     1   +(3/4)*1.41*y(6)*y(5))
dydx(3)=tau*(y(1)*y(2)-b*y(3)+2*y(4)*y(5))
```

```
dydx(4)=tau*(sigma*y(5)-(2)*sigma*y(4)
1  +(3/4)*1.41*y(1)*y(6))

dydx(5)=tau*(-2*y(5)-2*y(4)*y(3)+2*r*y(4)-(3/4)*1.41*y(6)*y(2)+
1   3*(1.41/4)*y(1)*y(7))
dydx(6)=tau*(-(3)*sigma*y(6)-(1/4)*1.41*y(1)*y(4)
1  +sigma*(1/3)*y(7))

dydx(7)=tau*(-(3/4)*1.41*y(4)*y(2)-3*(1.41/4)*y(1)*y(5)+2*r*y(6)
1 -3*y(7)-2*y(6)*y(8))
dydx(8)=tau*(2*y(6)*y(7)-4*b*y(8))
c
dydx(9)=tau*(sigma*y(17)-sigma*y(9)-(3/4)*1.41*y(6)*y(33)
1 -(3/4)*1.41*y(4)*y(49))
dydx(10)=tau*(sigma*y(18)-sigma*y(10)-(3/4)*1.41*y(6)*y(34)
1 -(3/4)*1.41*y(4)*y(50))
dydx(11)=tau*(sigma*y(19)-sigma*y(11)-(3/4)*1.41*y(6)*y(35)
1 -(3/4)*1.41*y(4)*y(51))
dydx(12)=tau*(sigma*y(20)-sigma*y(12)-(3/4)*1.41*y(6)*y(36)
1 -(3/4)*1.41*y(4)*y(52))
dydx(13)=tau*(sigma*y(21)-sigma*y(13)-(3/4)*1.41*y(6)*y(37)
1-(3/4)*1.41*y(4)*y(53))
```

```
dydx(14)=tau*(sigma*y(22)-sigma*y(14)-(3/4)*1.41*y(6)*y(38)
1 -(3/4)*1.41*y(4)*y(54))
dydx(15)=tau*(sigma*y(23)-sigma*y(15)-(3/4)*1.41*y(6)*y(39)
1 -(3/4)*1.41*y(4)*y(55))
dydx(16)=tau*(sigma*y(24)-sigma*y(16)-(3/4)*1.41*y(6)*y(40)
1 -(3/4)*1.41*y(4)*y(56))
c
dydx(17)=tau*((r-y(3))*y(9)-y(17)+(3/4)*1.41*y(7)*y(33)
1  +(3/4)*1.41*y(4)*y(57)+(3/4)*1.41*y(6)*y(41)
2  +(3/4)*1.41*y(5)*y(49))

dydx(18)=tau*((r-y(3))*y(10)-y(18)+(3/4)*1.41*y(7)*y(34)
1 +(3/4)*1.41*y(4)*y(58)+(3/4)*1.41*y(6)*y(42)
2 +(3/4)*1.41*y(5)*y(50))

dydx(19)=tau*((r-y(3))*y(11)-y(19)+(3/4)*1.41*y(7)*y(35)
1 +(3/4)*1.41*y(4)*y(59)+(3/4)*1.41*y(6)*y(43)
2 +(3/4)*1.41*y(5)*y(51))

dydx(20)=tau*((r-y(3))*y(12)-y(20)+(3/4)*1.41*y(7)*y(36)
1+(3/4)*1.41*y(4)*y(60)+(3/4)*1.41*y(6)*y(44)
2+(3/4)*1.41*y(5)*y(52))
```

```
dydx(21)=tau*((r-y(3))*y(13)-y(21)+(3/4)*1.41*y(7)*y(37)
1 +(3/4)*1.41*y(4)*y(61)+(3/4)*1.41*y(6)*y(45)
2 +(3/4)*y(5)*1.41*y(53))

dydx(22)=tau*((r-y(3))*y(14)-y(22)+(3/4)*1.41*y(7)*y(38)
1 +(3/4)*1.41*y(4)*y(62)+(3/4)*1.41*y(6)*y(46)
2 +(3/4)*y(5)*1.41*y(54))

dydx(23)=tau*((r-y(3))*y(15)-y(23)+(3/4)*1.41*y(7)*y(39)
1+(3/4)*1.41*y(4)*y(63)+(3/4)*1.41*y(6)*y(47)
2+(3/4)*y(5)*1.41*y(55))

dydx(24)=tau*((r-y(3))*y(16)-y(24)+(3/4)*1.41*y(7)*y(40)
1+(3/4)*1.41*y(4)*y(64)+(3/4)*1.41*y(6)*y(48)
2+(3/4)*1.41*y(5)*y(56))

c
dydx(25)=tau*(y(2)*y(9)+y(1)*y(17)-b*y(25)+2*y(5)*y(33)
1   +2*y(4)*y(41))
```

```
dydx(26)=tau*(y(2)*y(10)+y(1)*y(18)-b*y(26)+2*y(5)*y(34)
1  +2*y(4)*y(42))



dydx(27)=tau*(y(2)*y(11)+y(1)*y(19)-b*y(27)+2*y(5)*y(35)
1 +2*y(4)*y(43))
dydx(28)=tau*(y(2)*y(12)+y(1)*y(20)-b*y(28)+2*y(5)*y(36)
1 +2*y(4)*y(44))
dydx(29)=tau*(y(2)*y(13)+y(1)*y(21)-b*y(29)+2*y(5)*y(37)
1 +2*y(4)*y(45))
dydx(30)=tau*(y(2)*y(14)+y(1)*y(22)-b*y(30)+2*y(5)*y(38)
1+2*y(4)*y(46))
dydx(31)=tau*(y(2)*y(15)+y(1)*y(23)-b*y(31)+2*y(5)*y(39)
1 +2*y(4)*y(47))
dydx(32)=tau*(y(2)*y(16)+y(1)*y(24)-b*y(32)+2*y(5)*y(40)
1 +2*y(4)*y(48))
c
dydx(33)=tau*((3/4)*1.41*y(6)*y(9)-2*sigma*y(33)
1 +sigma*y(41)+(3/4)*1.41*y(1)*y(49))
dydx(34)=tau*((3/4)*1.41*y(6)*y(10)-2*sigma*y(34)
1 +sigma*y(42)+(3/4)*1.41*y(1)*y(50))
dydx(35)=tau*((3/4)*1.41*y(6)*y(11)-2*sigma*y(35)
```

```
1 +sigma*y(43)+(3/4)*1.41*y(1)*y(51))
dydx(36)=tau*((3/4)*1.41*y(6)*y(12)-2*sigma*y(36)
1 +sigma*y(44)+(3/4)*1.41*y(1)*y(52))
dydx(37)=tau*((3/4)*1.41*y(6)*y(13)-2*sigma*y(37)
1 +sigma*y(45)+(3/4)*1.41*y(1)*y(53))
dydx(38)=tau*((3/4)*1.41*y(6)*y(14)-2*sigma*y(38)
1 +sigma*y(46)+(3/4)*1.41*y(1)*y(54))
dydx(39)=tau*((3/4)*1.41*y(6)*y(15)-2*sigma*y(39)
1 +sigma*y(47)+(3/4)*1.41*y(1)*y(55))
dydx(40)=tau*((3/4)*1.41*y(6)*y(16)-2*sigma*y(40)
1 +sigma*y(48)+(3/4)*1.41*y(1)*y(56))
c
dydx(41)=tau*(3*(1.41/4)*y(7)*y(9)-(3/4)*1.41*y(6)*y(17)
1  -2*y(4)*y(25)+2*(r-y(3))*y(33)-2*y(41)
2  -(3/4)*1.41*y(2)*y(49)+3*(1.41/4)*y(1)*y(57))

dydx(42)=tau*(3*(1.41/4)*y(7)*y(10)-1.41*(3/4)*y(6)*y(18)
1 -2*y(4)*y(26)+2*(r-y(3))*y(34)-2*y(42)
2 -(3/4)*1.41*y(2)*y(50)+3*(1.41/4)*y(1)*y(58))

dydx(43)=tau*(3*(1.41/4)*y(7)*y(11)-(3/4)*1.41*y(6)*y(19)
1    -2*y(4)*y(27)+2*(r-y(3))*y(35)-2*y(43)
```

```
2 -(3/4)*1.41*y(2)*y(51)+3*(1.41/4)*y(1)*y(59))
dydx(44)=tau*(3*(1.41/4)*y(7)*y(12)-(3/4)*1.41*y(6)*y(20)
1   -2*y(4)*y(28)+2*(r-y(3))*y(36)-2*y(44)
2 -(3/4)*1.41*y(2)*y(52)+3*(1.41/4)*y(1)*y(60))
dydx(45)=tau*(3*(1.41/4)*y(7)*y(13)-(3/4)*(1.41)*y(6)*y(21)
1 -2*y(4)*y(29)+2*(r-y(3))*y(37)-2*y(45)
2 -(3/4)*1.41*y(2)*y(53)+3*(1.41/4)*y(1)*y(61))

dydx(46)=tau*(3*(1.41/4)*y(7)*y(14)-(3/4)*1.41*y(6)*y(22)
1 -2*y(4)*y(30) +2*(r-y(3))*y(38)-2*y(46)
2-(3/4)*1.41*y(2)*y(54)+3*(1.41/4)*y(1)*y(62))

dydx(47)=tau*(3*(1.41/4)*y(7)*y(15)-(3/4)*1.41*y(6)*y(23)
1 -2*y(4)*y(31)+2*(r-y(3))*y(39)-2*y(47)
2-(3/4)*1.41*y(2)*y(55)+3*(1.41/4)*y(1)*y(63))

dydx(48)=tau*(3*(1.41/4)*y(7)*y(16)-(3/4)*1.41*y(6)*y(24)
1 -2*y(4)*y(32)+2*(r-y(3))*y(40)-2*y(48)
2 -(3/4)*1.41*y(2)*y(56)+3*(1.41/4)*y(1)*y(64))
c
dydx(49)=tau*(-3*(1/4)*1.41*y(4)*y(9)-(1/4)*1.41*y(1)*y(33)
1 -3*sigma*y(49)+(1/3)*sigma*y(57))
```

```
dydx(50)=tau*(-3*(1/4)*1.41*y(4)*y(10)-(1/4)*1.41*y(1)*y(34)
1 -3*sigma*y(50)+(1/3)*sigma*y(58))
dydx(51)=tau*(-3*(1/4)*1.41*y(4)*y(11)-(1/4)*1.41*y(1)*y(35)
1 -3*sigma*y(51)+(1/3)*sigma*y(59))
dydx(52)=tau*(-3*(1/4)*1.41*y(4)*y(12)-(1/4)*1.41*y(1)*y(36)
1 -3*sigma*y(52)+(1/3)*sigma*y(60))
dydx(53)=tau*(-3*(1/4)*1.41*y(4)*y(13)-(1/4)*1.41*y(1)*y(37)
1 -3*sigma*y(53)+(1/3)*sigma*y(61))
dydx(54)=tau*(-3*(1/4)*1.41*y(4)*y(14)-(1/4)*1.41*y(1)*y(38)
1 -3*sigma*y(54)+(1/3)*sigma*y(62))
dydx(55)=tau*(-3*(1/4)*1.41*y(4)*y(15)-(1/4)*1.41*y(1)*y(39)
1 -3*sigma*y(55)+(1/3)*sigma*y(63))
dydx(56)=tau*(-3*(1/4)*1.41*y(4)*y(16)-(1/4)*1.41*y(1)*y(40)
1 -3*sigma*y(56)+(1/3)*sigma*y(64))
c
dydx(57)=tau*(-3*(1.41/4)*y(5)*y(9)-(3/4)*1.41*y(4)*y(17)
1 -(3/4)*1.41*y(2)*y(33)+2*(r-y(8))*y(49)
2 -3*(1.41/4)*y(1)*y(41)-3*y(57)-2*y(6)*y(65))

dydx(58)=tau*(-3*(1.41/4)*y(5)*y(10)-(3/4)*1.41*y(4)*y(18)
1 -(3/4)*1.41*y(2)*y(34)+2*(r-y(8))*y(50)
2 -3*(1.41/4)*y(1)*y(42)-3*y(58)-2*y(6)*y(66))
```

```
dydx(59)=tau*(-3*(1.41/4)*y(5)*y(11)-(3/4)*1.41*y(4)*y(19)
1 -(3/4)*1.41*y(2)*y(35)+2*(r-y(8))*y(51)
2 -3*(1.41/4)*y(1)*y(43)-3*y(59)-2*y(6)*y(67))

dydx(60)=tau*(-3*(1.41/4)*y(5)*y(12)-(3/4)*1.41*y(4)*y(20)
1 -(3/4)*1.41*y(2)*y(36)+2*(r-y(8))*y(52)
2 -3*(1.41/4)*y(1)*y(44)-3*y(60)-2*y(6)*y(68))

dydx(61)=tau*(-3*(1.41/4)*y(5)*y(13)-(3/4)*1.41*y(4)*y(21)
1 -(3/4)*1.41*y(2)*y(37)+2*(r-y(8))*y(53)
2 -3*(1.41/4)*y(1)*y(45)-3*y(61)-2*y(6)*y(69))

dydx(62)=tau*(-3*(1.41/4)*y(5)*y(14)-(3/4)*1.41*y(4)*y(22)
1 -(3/4)*1.41*y(2)*y(38)+2*(r-y(8))*y(54)
2 -3*(1.41/4)*y(1)*y(46)-3*y(62)-2*y(6)*y(70))

dydx(63)=tau*(-3*(1.41/4)*y(5)*y(15)-(3/4)*1.41*y(4)*y(23)
1 -(3/4)*1.41*y(2)*y(39)+2*(r-y(8))*y(55)
2 -3*(1.41/4)*y(1)*y(47)-3*y(63)-2*y(6)*y(71))

dydx(64)=tau*(-3*(1.41/4)*y(5)*y(16)-(3/4)*1.41*y(4)*y(24)
```

```
1 -(3/4)*1.41*y(2)*y(40)+2*(r-y(8))*y(56)
2 -3*(1.41/4)*y(1)*y(48)-3*y(64)-2*y(6)*y(72))

c
dydx(65)=tau*(2*y(7)*y(49)+2*y(6)*y(57)-4*b*y(65))
dydx(66)=tau*(2*y(7)*y(50)+2*y(6)*y(58)-4*b*y(66))
dydx(67)=tau*(2*y(7)*y(51)+2*y(6)*y(59)-4*b*y(67))
dydx(68)=tau*(2*y(7)*y(52)+2*y(6)*y(60)-4*b*y(68))
dydx(69)=tau*(2*y(7)*y(53)+2*y(6)*y(61)-4*b*y(69))
dydx(70)=tau*(2*y(7)*y(54)+2*y(6)*y(62)-4*b*y(70))
dydx(71)=tau*(2*y(7)*y(55)+2*y(6)*y(63)-4*b*y(71))
dydx(72)=tau*(2*y(7)*y(56)+2*y(6)*y(64)-4*b*y(72))


return
end
c
c      subroutine ornorm constructs a new orthonormal basis by the
c gram-schmidt method
c
        subroutine ornorm(nle,y,cum,gsc,znorm,ex,t)
        real znorm(nle),y(72),gsc(nle),cum(nle),ex(nle),t
```

```
      integer j,nle,ne,k,l
      common ne
c     normalize first vector
      znorm(1)=0.0
      do 30 j=1,nle
      znorm(1)=znorm(1)+y(nle*j+1)**2
30    continue
      znorm(1)=sqrt(znorm(1))
      do 40 j=1,nle
      y(nle*j+1)=y(nle*j+1)/znorm(1)
40    continue
c     generate a new set of orthonormal vectors

      do 80 j=2,nle
c generate j-1 gsr coefficients
      do 50 k=1,j-1
      gsc(k)=0.0
      do 50 l=1,nle
      gsc(k)=gsc(k)+y(nle*l+j)*y(nle*l+k)
50    continue
c     construct a new vector
```

```
      do 60 k=1,nle
      do 60 l=1,(j-1)
       y(nle*k+j)=y(nle*k+j)-gsc(l)*y(nle*k+l)
60     continue
c   calculate vectors norm

znorm(j)=0.0
do 70 k=1,nle
znorm(j)=znorm(j)+y(nle*k+j)**2
70     continue
      znorm(j)=sqrt(znorm(j))
c    normalize the new vector
      do 80 k=1,nle
      y(nle*k+j)=y(nle*k+j)/znorm(j)
80     continue
c    update vector magnitudes
     do 90 k=1,nle
     cum(k)=cum(k)+alog(znorm(k))/alog(2.0)
     ex(k)=cum(k)/t
c    write(*,*) t,ex(k)
90     continue
       return
```

```
end
```

APPENDIX C

MATLAB CODE TO INTEGRATE ODES

```
Program lorenz5d
Implicit none
c this program solves 5d Lorenz system
c declarations
c n: number of equations, min/max in x, dist: length of x-steps
c y(1): initial position, y(2):initial velocity
Real*8Tau, y(5),sigma,b,R,xdat,ydat,zdat,t,sdat,wdat,vdat,v1dat
Real*8 w1dat, s1dat
c       real*8 h, e, left, right, k, dist, de
        Integer n, i, ij
        parameter(n=8192,tau=0.005,b=8.0/3.0)
        data sigma,r/10.d0,15.0d0/
c     set initial conditions



c
c       eps=0.0001 !tolerance value for our result



        y(1)=10
        y(2)=5
```

```
      y(3)=20
      y(4)=15
      y(5)=30
c     y(6)=35
c     y(7)=15
c     y(8)=10
c     y(9)=25
c     de=0.01



c     do n steps of Runga-Kutta algorithm
c     from right and also from left
      Do 100 ij=1,n
      t=0.0d0
      Call rk4(tau,r,sigma,b,y)

      t=float(ij)*tau

      do 50 i=1,9
       if(i.eq.1)then
```

```
        xdat=y(1)
        elseif(i.eq.2)then
        ydat=y(2)
        elseif(i.eq.3)then
        zdat=y(3)
        elseif(i.eq.4)then
        vdat=y(4)
        elseif(i.eq.5)then
        wdat=y(5)
c       elseif(i.eq.6)then
c       sdat=y(6)
c       elseif(i.eq.7)then
c       v1dat=y(7)
c       elseif(i.eq.8)then
c       w1dat=y(8)
c       elseif(i.eq.9)then
c       s1dat=y(9)
        endif
50      continue
      open(unit=10,file='lore1.dat',status='unknown')
      write(10,*)xdat,ydat,zdat
100   continue
```

```
      stop
      end

c------------------------end of main program----------------------
c
c fourth-order Runge-Kutta subroutine
      Subroutine rk4(tau,r,sigma,b, y)
      Implicit none
c declarations
      Real*8 dydx(5),tau,y1(5),dydx2(5),dydx3(5)
      real*8   y(5),dydx4(5),r,sigma,b
Integer i
call dervs(y,dydx,r,sigma,b,tau)
Do 10 i = 1,5
y1(i) = y(i)+0.5d0 *dydx(i)
 10    Continue
      call dervs(y1,dydx2,r,sigma,b,tau)
      Do 20 i = 1,5
```

```
        y1(i) = y(i)+0.5d0*dydx2(i)

 20     Continue
        call dervs(y1,dydx3,r,sigma,b,tau)
        Do 30 i = 1,5
          y1(i) = y(i)+dydx3(i)

 30     Continue
        call dervs(y1,dydx4,r,sigma,b,tau)
        Do 40 i = 1,5

     y(i) = y(i) + (dydx(i) + (2.*(dydx2(i) + dydx3(i)))+dydx4(i))/6.0
 40     Continue
c
        Return
        End
c function which returns the derivatives
        subroutine dervs(y,dydx,r,sigma,b,tau)
        Implicit none
c       declarations
        Real*8 y(5),dydx(5),r,sigma,b,tau
```

```
dydx(1)=tau*(-sigma*y(1)+sigma*y(2))

dydx(2)=tau*(-y(1)*y(3)+r*y(1)-y(2))

dydx(3)=tau*(y(1)*y(2)+2*y(4)*y(5)-b*y(3))

dydx(5)=tau*(-2*y(4)*y(3)+2*r*y(4)-2*y(5))

dydx(4)=tau*(sigma*y(5)-2*sigma*y(4))
return

end
```

APPENDIX D

MATLAB CODE FOR POWER SPECTRA

program on power spectra

```
load roy1.dat;

n=8192;

xdat=roy1(1:n,1);

ydat=roy1(1:n,2);

zdat=roy1(1:n,3);

fx=fft(xdat,n);

pxx=fx.*conj(fx)/n;

f=1000*(0:((n/2)-1))/n;

px=log10(pxx);

plot(f,px(1:(n/2)),'k');

axis([0 50 -5 5]);

title('power spectrum for lorenz 8d');

xlabel('hz','fontsize',15);

ylabel('log10(power)','fontsize',15);

set(gca,'fontsize',13,'x color','black','y color','black','z color','black')
```

REFERENCES

[1] Poincare , H. Acta Mathematica. Vol. 7, pp. 259-380(1885)

[2] Landau,L.D. Dokl.Akad.Nauk SSSR. Vol.44.pp. 339-342(1944)

[3] Malkus, W.V.R; G. Veronis. J.Fluid Mech. Vol.4,pp.225-260(1958)

[4] Kuo , H.L. 1961. J. Fluid. Mech. Vol. 10, pp. 611-634

[5] Von Neumann, 1961. J John von Neumann Collected works. Ed.Taub,A.H., Pergamon Press, New York.

[6] B. Saltzman, J. Atmos. Sci. 19. pp. 329-341 (1962).

[7] E.N. Lorenz, J. Atmos. Sci.20.pp. 130-141 (1963).

[8] Ruelle , D., F.Takens. 1971. Commun.Math.Phys. Vol.20,pp. 167-192

[9] J.H. Curry, Commun. Math, Phys.60, 193 (1978).

[10] J.H. Curry, SIAM J. Math. Anal.10, 71 (1979).

[11] L.N. Howard, and R.K. Krishnamurti, J. Fluid Mech.170, 385 (1986).

[12] J.M.T. Thompson, and H.B. Stewart, Nonlinear Dynamics and Chaos (New York weily & Sons Ltd, 1986).

[13] E.A. Jackson, Perspectives of Nonlinear Dynamics (Cambridge, Cambridge uni.press 1990), Vol. 2, 138.

[14] R.C. Hilbron, Chaos and Nonlinear Dynamics (Oxford, Oxford Uni. Press, (1994)

[15] K.S. Kennamer, M.S. Thesis The University of Alabama in Huntsville (1995)

[16] J.L. Thieffault and W. Horton, Phys. Fluids 8, 1715 (1996).

[17] P. Reiterer, C. Lainscsek, F. Schurrer, C. Letellier and J. Maquet, J. Phys. A:Math Gen. 31, 7121 (1998).

[18] C. Tong and A. Gluhovsky, Phys. Rev. E 65 , 046306-1-11 (2002).

[19] M. Humi, arXiv:nlin.CD/0409025 v1 (2004).

[20] G.Chen, and D.Cheng, Int. J. Bifurcation and Chaos 14, 1507 (2004).

[21] D.E. Musielak, Z.E. Musielak, and K.S. Kennamer, Fractals 13, 19 (2005).

[22] Z.-M. Chen and W.G. Price, Chaos, Solitons and Fractals 28, 571 (2006).

[23] D. Roy, and Z.E. Musielak, Chaos, Solitons and Fractals, in press (2006) - I

[24] D.Roy, and Z.E.Musielak,Chaos,solitons and Fractals, in press(2006) –II

[25] D.Roy, and Z.E.Musielak, Chaos, solitons and Fractals, in press (2006) –III

BIOGRAPHICAL INFORMATION

The author was born in Kolkata, INDIA. He received his master's degree from University of Pune and IIT Bombay. He has been a graduate student at the physics department of the University of Texas at Arlington from fall 04 till spring 06.